Drone-Based VOC Sampling System for Atmospheric Insights in the Amazon

Acknowledgements

I would like to thank Karena McKinney for her guidance on defining scientific requirements, system design, and engineering validation. Special thanks to Rob Wood for valuable feedback and Scot Martin for supporting this project and its future applications in the Amazon. In addition, I would like to thank Terry Martin and Marco Rivero for their assistance with engineering design.

Special thanks to Brandon Montellato (DJI), Anas Chalah, and Steve Cortesa for their help in acquiring a drone for conducting test flights.

Lastly, I would like to thank my friends, family, and fellow ES100 engineering students for their support and encouragement in times of need.

Abstract

Produced mainly through natural emission from vegetation (~10^{15} grams a year), volatile organic compounds (VOCs) influence climate through their involvement in photochemistry, such as the production of ozone in the presence of NO_x and light. Decades of stationary tower-based studies (~10s of meters) and aircraft flights (~10s of kilometers) have revealed extreme heterogeneity in VOC concentrations in time and space. However, the actual variation in forest cover occurs at ~1 km and less, a scale that represents a missing link in our present-day understanding of VOCs in atmospheric chemistry. This project involves the engineering design, production, and validation of a drone-deployed VOC sampling instrument. The instrument design includes a custom pump and selector valve system for sequentially collecting samples through multiple sorbent-packed thermal desorption tubes and features a lightweight enclosure that can be integrated directly to the chassis of existing drone platforms. Component validation tests revealed high flow rate consistency and no significant gas leakage, both important requirements for post-flight gas chromatography analysis. An onboard microcontroller successfully controlled sampling routines and flow system data acquisition and storage to an onboard memory card. Furthermore, flight tests with the sampler instrument integrated to a DJI Matrice 600 drone demonstrated unimpaired flight dynamics as well as full flow system function under a series of flight maneuvers in high winds. Once deployed as part of a multi-drone fleet from a mobile boat platform, this sampling instrument will help elucidate uncertainties surrounding the magnitudes, variations, and processes controlling VOC emission and uptake at previously unexplored spatial and temporal scales.

Table of contents

List of figures

List of tables

Chapter 1

Introduction

1.1 Background

Volatile organic compounds (VOCs) are organic chemicals that vaporize readily at room temperature. Over the past three decades, the role of VOCs in tropospheric photochemistry has been the focus of major research efforts, including within the context of assessing air quality at the junction of urban cities and forested regions. While the regional and global impacts of anthropogenic sources of VOCs – such as fuel production and biomass burning – have increased steadily in recent years, natural emission from vegetation (biogenic volatile organic compounds, or BVOCs) remains the most significant source of VOC generation, with annual emissions accounting for 1.15 petagrams (10^{15}) of carbon in the form of VOCs [6].

With short atmospheric lifetimes, VOCs influence climate through the production of organic aerosols and their involvement in tropospheric photochemistry, such as the production of ozone in the presence of NO_x and light. Excess levels of BVOCs or NO_x can cause an imbalance in such reactions and cause secondary photochemical pollution, leading to elevated ozone generation that can have detrimental effects on human health [14] and crop yields [8]. Furthermore, various BVOCs are known to be directly involved in complex signaling pathways in response to plant stress and trauma [15]. Of particular interest is the fact that increased emissions of certain BVOCs are associated with plants experiencing environmental stress [9]. Given the major role BVOCs have in photochemistry and ecological systems, a better understanding of the spatial and temporal patterns of VOC concentrations in areas of dense vegetation – such as the Amazon rainforest –

will serve as an important indicator of ecosystem stability, elucidate complex ecological relationships between rainforest species, and provide new insight into the chemical mechanisms behind climate change.

1.2 Current Challenges

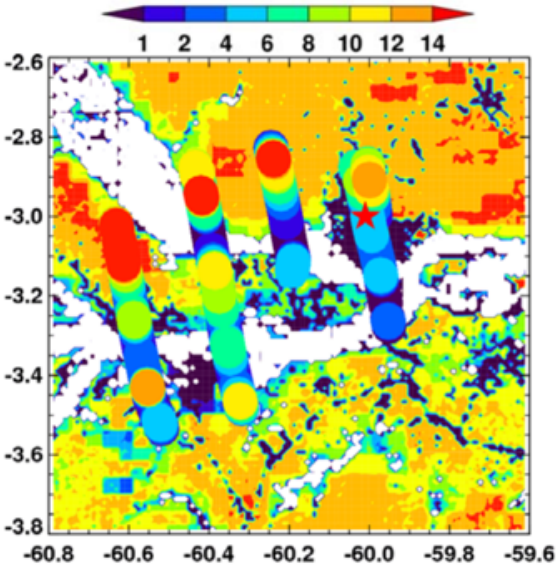

Fig. 1.1 **Heterogeneity of isoprene emissions with land cover.** The background color map shows isoprene fluxes ($mg \cdot m^{-2} \cdot h^{-1}$), reflecting variation in land cover, while the foreground color map shows aircraft recorded isoprene fluxes measured in September 2014. The white shows a major tributary in the Amazon river system. The red star indicates Manaus, Brazil. Scale: 0.1°= 11km. [7]

In recent years, many research efforts on these fundamental questions have been hindered as a result of the recent recognition of extreme VOC heterogeneity in time and space, which existing measurement platforms are unable to capture. For instance, Figure 1.1 shows the heterogeneity of modeled isoprene fluxes in the background coloring and aircraft-measured isoprene fluxes in the foreground for a major tributary system in the Amazon rainforest [7]. Historically, BVOC emission research has utilized sensors on fixed tower platforms, short-term airborne surveys using fast-flying aircraft high in the boundary layer, tethered balloon systems, and satellite-based sensors. However, each of these methods come with unique limitations. For instance, fixed tower sensors are costly and difficult to construct in dense forested regions. They also fail to provide dynamic spatial and temporal flexibility. Tethered balloon surveys are notoriously difficult to control

and aircraft missions typically take place at altitudes at which target BVOCs have been partially or completely consumed by photochemical reactions. Lastly, satellite-based sensors are only able to provide coarse resolution measurements with low temporal flexibility. Despite these challenges, decades of stationary tower-based studies (~10s of meters) and aircraft flights (10s of kilometers) have still revealed great variability in VOC levels across different forest regions and that the most reactive VOC species are depleted before reaching aircraft altitudes. However, the actual variation in forest cover is on the scale of 1 km and less. This scale, reflecting the primary range for VOC emission and uptake, is not represented in current VOC data sets, yet is precisely the missing link in advancing our present-day understanding of VOCs in atmospheric chemistry.

1.3 Benefits

In light of these limitations, recent advancements in drone technologies present an emerging frontier in atmospheric chemistry, promising a new generation of scientific platforms that can collect data sets at previously unexplored scales. This project involves the mechanical design, assembly, and field validation of a flight-ready VOC sampling instrument to be integrated with a research grade drone (DJI Matrice 600 or similar). The instrument design includes a custom constant flow-rate pump and selector valve system for collecting samples through multiple adsorbent thermal desorption (ATD) cartridges. These tubed cartridges trap specific VOCs onto a sorbent matrix as an air sample is pumped through the tube. After collection, the ATD cartridges will be analyzed onboard a mobile boat platform traveling through the waterways of the Amazon rainforest. The cartridges are processed via thermal desorption, an analytical method that utilizes heat to volatilize trapped VOCs from the solid matrix for separation and analysis by gas chromatography. With a payload of just ~1 kg., modular form factor, and flight time of ~30 minutes for six sampling sites, the instrument meets engineering specifications that align perfectly with the operating capabilities of DJI's Matrice drone series. The instrument will be outfitted to mate with the Matrice drone payload platform.

Together with the flight capabilities offered by modern day drone platforms, this instrument will open the door to studying VOC emission and uptake at previously inaccessible scales. In the long term, data from this project will shed

light on atmospheric chemistry, biodiversity, and ecosystem stress within the context of global climate change.

Chapter 2

Objectives and Goals

2.1 Scientific Requirements

BVOCs are highly diverse and attempts at classification by modern studies have led to multiple subgroups [16],[17],[5]. In general, these groupings include:

1. numerous terpenes including isoprene (C_5H_8), monoterpenes ($C_{10}H_{16}$), and sesquiterpenes ($C_{15}H_{24}$)
2. terpenes that are functionalized (i.e. oxidixed)
3. alkanes and alkenes
4. oxygenated species (alkyl aldehydes, ketones, alkyl alcohols, ethers, acids, and esters)

The BVOCs of interest at the target deployment sites in the Amazon presented in this study will primarily be plant-produced compounds and their early oxidation products. Various sampling and analytical methodologies for resolving BVOC emissions have been developed to serve a wide array of scientific research objectives. In particular, field-deployed instrumentation has been successfully utilized in recent years for studies involving plant-derived BVOCs in ambient air, where emissions and ambient concentrations are subject to short time variations. As summarized in Table 2.1, such studies include in situ analytical instruments with integrated gas sampling as well as systems limited to sample collection for off-site analysis.

Table 2.1 Past studies involving the survey of biogenic VOC concentrations. Minimum detection limits for isoprene are shown for various methods of collection and detection.

	Langford et al. (2010) [10]	Mielke et al. (2010) [11]	Mitstzal et al. (2010) [12]	Pankow, et al. (2012) [13]	Chang et al. (2016) [4]
collection method	direct inlet	direct inlet	ATD cartridge, 1 L	ATD cartridge, 5 L	whole air sampler, 2 L
detection method	proton transfer reaction mass spectrometry (PTR-MS)	proton transfer reaction mass spectrometry (PTR-MS)	gas chromatograpy-mass spectrometry (GC/MS)	Two dimensional gas chromatography (GC _ GC) with detection by time-of-flight mass spectrometry (TOFMS)	gas chromatography-flame ionization detector (GC/-FID)
sampling location	Sabah, Malaysia	Michigan, USA	Sabah, Malaysia	Colorado, USA	Taiwan
minimum detection limit (MDL) for isoprene [pptv]	200	93	100	3.5	3

Major drone and UAV platform manufacturers (i.e. DJI, Yuneec, etc.) typically divide their product lines between consumer- and industrial-grade platforms. Compared to consumer-grade models, industrial platforms typically offer increased payload capacities, extended flight times (several hours to several days), and the option of mounting custom hardware. Still, overall flight capabilities are typically limited to 30 minutes with a 2-5kg payload with even top model commercial-off-the-shelf (COTS) drones, preventing missions with sampling methodologies that require extended exposure or collection times. Given the payload and flight time capabilities of candidate drone platforms (i.e. DJI Matrice 600 and 100) for in situ sampling in the Amazon rainforest, adsorption/thermal desorption (ATD) cartridge sampling of a known air volume followed by thermal desorption of the analytes to a field GC instrument was selected as the sampling methodology for the design of the instrument presented in this study. Thermal desorption is an analytical technique that utilizes heat to volatilize analytes such that they can be separated from a solid sorbent matrix. ATD cartridges are lightweight and provide a simple, sensitive, and quantitative approach for determining a wide range of VOCs at ambient atmospheric levels through both pumped and diffusive (passive) sampling. Furthermore, cartridges can easily be sealed after sampling and transported for off-site analysis. These versatile features make sampling with ATD cartridges coupled with a gas chromatography instrument the ideal method of BVOC collection for a drone-based sampling platform.

ATD cartridge sampling requires a pump with a calibrated flow rate in order to determine the volume captured throughout the sampling period. A constant low volumetric flow rate (0.1-0.4 L/min based on past studies) is desired to allow for optimal sorbent-sorbate interaction and uptake into the sorbent matrix. Based on the relationship between sample volume and minimum detection limit reported by past studies, a target sampling volume of 1.0 L per ATD cartridge collected at a constant flow rate of 175 sccm was defined. This results in about 5 minutes of sampling time per ATD cartridge, which results in a minimum required flight time of 30 minutes in order to sample with 5 ATD cartridges while also carrying out take-off/landing and transits between sampling locations. ATD cartridges should be oriented in a vertical position for sampling since horizontal installation can cause “channeling” to occur as a result of sorbent falling away from the walls of the ATD cartridge.

2.2 Engineering Goals

The mechanical and electrical design objectives for the absorbent cartridge sampler instrument are mainly dictated by the functional performance specifications of the Matrice 600 platform within the context of mission requirements. In particular, proposed flight plans within the Amazon will extend horizontally from riparian to several kilometers inland and vertically from near canopy to several hundred meters in height. Such sampling trajectories will allow specific sub-types of the rainforest to be targeted at scales of 1 km or less. Operation of the drones will take place from a boat that will be continuously re-positioned along the Amazon river system, allowing for sampling flights spanning a range of different heterogeneous forest types in the Amazonia.

These mission objectives will require the sampler instrument to differentially activate multiple ATD cartridges during a single flight program in order to collect multiple VOC samples. Given the flow rate and minimum sample volume requirements per ATD cartridge, the mass of the instrument directly dictates the upper bound of the achievable flying time per flight program. Equivalently, since the sampling time per ATD cartridge is fixed, the mass of the instrument - combined with the capabilities of the drone platform itself - determines the number of ATD cartridges that can be deployed per flight program.

A summary of the scientific and engineering design goals for the instrument are shown in Table 2.2. In particular, given a 175 sccm target volumetric flow rate, 5.71 minutes are required at each GPS waypoint for a total of 1.0 L of sampled air per ATD cartridge. This results in 28.55 minutes of total sampling time. The Matrice 600 is rated for 35.0 minutes of hover time with no payload and 16.0 minutes with a 6.0 kg. payload (using the six provided TB47S batteries). It is important to note that these values are strictly for hovering in a controlled environment, and that actual flight times are highly variable based on ambient flight conditions (wind, temperature, etc.). A linear equation based on these two data points (35.0 minutes for no payload and 16.0 minutes for a 6.0 kg payload) was used to interpolate estimated total flight time based on payload mass. Based on this calculation and estimated weight requirements for the instrument components, a maximum instrument mass of < 5.0 lbs. was selected as an engineering goal in order to ensure sufficient flight time for sampling from multiple ATD cartridges.

Table 2.2 General engineering design and scientific requirements.

Specification/Requirement	Target Value	Achieved Value	Units
Mass	<5 lbs.	1.95	lbs
Volume	8 x 8 x 12	7.45 x 8 x 2	in
Power	External or drone battery	Drone battery	–
Flight time	∼30	∼36	min
Specificity (Minimum Detection Level)	100 pptv (based on past studies)	To be determined by future flights in the Amazon	pptv
Volume	0.25 - 1.0	1.0	L
Flow	∼100-400 constant flow	∼175	sccm

Chapter 3

System Design

3.1 Design Approach

The overarching system design of the instrument is intended to fit a standalone, modular form factor in order to simplify installation and troubleshooting as well as to maximize electromechanical compatibility with multiple drone platforms in the field. The instrument resides in a rectangular casing that can be opened for easy access for repairs and software updates to the onboard Arduino Uno microcontroller. The individual components of the flow system are arranged in a linear configuration from the bow to stern of the drone. Electrical components are stacked vertically in order to reduce the overall footprint of the instrument. The casing does not need to be opened or disassembled from the chassis of the drone platform in order to load new ATD cartridges prior to each flight program. Moreover, the instrument casing is directly integrated to the underside of the drone chassis and does not interfere with standard flight operations, including the functionality of the Matrice 600's automatically retracting landing legs.

Figure3.1 shows the full system schematic, including major analog and digital electrical connections (shown in orange and green, respectively) as well as pump system flow paths (shown in blue). The entire system can either be powered by the 18.0 VDC output provided by the power distribution board (PDB) onboard the Matrice 600 or an external battery pack, the tradeoffs for which will be discussed in detail in a subsequent section. Two voltage regulators provide 5 and 24 VDC outputs for the pump, sensors, valve manifold, and driver boards. Air is drawn through the instrument at constant volumetric flow rate by a diaphragm pump positioned downstream from the rest of the components in

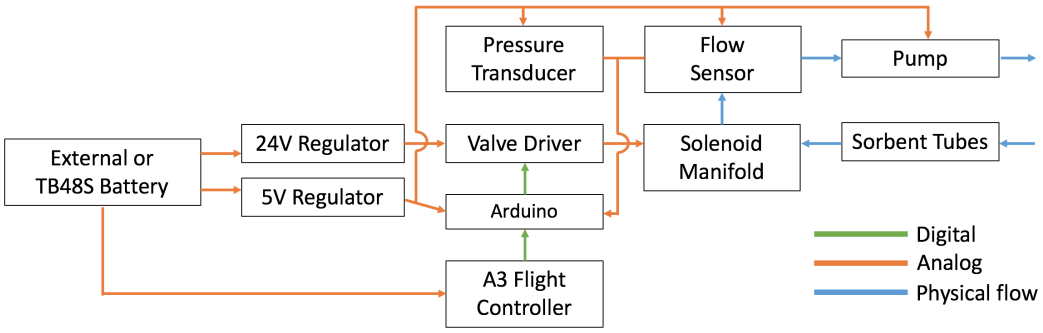

Fig. 3.1 **System diagram of sampling instrument.** All instrument components are powered by the drone's onboard batteries and are controlled by an Arduino Uno microcontroller. Gas flows in through the ATD cartridges (sorbent tubes) and out of the pump.

the flow system. Placing the ATD cartridges at the upstream position ensures that sample gas always passes through cartridges before entering the remainder of the flow system, thus preventing potential contamination from the flow system tubing.

An Arduino Uno serves as the digital interface between the Matrice 600's flight computer and the control of the instrument. Specifically, the Uno coordinates the activation and operation of the pump, sensors, and valves.

3.2 Component Level Details

3.2.1 Flow System Tubing

Two types of tubing are used throughout the flow system in order to provide compatibility between each of the components. 1/8" ID x 1/4" OD x 1/16" Wall Tygon® Ultra Chemical Resistant Tubing is used between all flow components with the exception of the solenoid valve manifold. The polyolefin-based tubing is chemically inert and its high flexibility makes it an ideal candidate for the compact shape of the instrument. The manual orifice valve is attached directly to the Tygon tubing downstream of the diaphragm pump.

All tubing connected directly to the solenoid valve manifold is 1/16" ID x 1/8" OD x 1/32" Wall Teflon tubing. The ends of the tubing feeding directly into

the valve manifold were flanged and installed with washers to ensure a leak-proof fit. PTFE 1/4” x 1/8” reducing unions were used to connect the nylon and Tygon tubes as well as the nylon tubing and the ATD cartridges (1/4" OD).

The conductance of the flow system was calculated to ensure that the diaphragm pump would be able to support the pressure drop across the system. Specifically, the conductance of each segment of tubing was modeled as a viscous flow regime and the total conductance of the tubing was used to calculate the pressure drop between the inlet and outlet of the flow system. The total conductance for the system, modeled as n sections of tubing in series, is given by:

$$\frac{1}{C_{total}} = \frac{1}{C_1} + \frac{1}{C_2} + \frac{1}{C_3} + \cdots + \frac{1}{C_n}$$

For a system in a steady-state viscous flow regime, the total conductance for the system is related to the volumetric flow rate by:

$$C_{total} = \frac{Q}{P_1 - P_2} = [\frac{\pi D^4}{128\eta L}] \times P = 182 \times \frac{D^4}{L} \times \overline{p}$$

In this equation, Q is throughput [torr]$\cdot$ [cm]/[s], $P1$ is the downstream pressure [torr] (measured at the exit), $P2$ is the upstream pressure [torr] (measured at the entrance), D is the inner diameter of the tube [cm], L is the length of tubing [cm], and $\overline{p}$ is the average pressure between the inlet and outlet of the length of tubing [torr]. Using the above equation, the conductance for the segment of 1/4" ID Tygon tubing from the pump to atmosphere can be calculated. Note that the pressure drop was estimated for a cylindrical tube with irrotational, axisymmetric, and steady-state flow. The viscosity of air at 25°C is 1.845×10^{-4} poise = 1.845×10^{-5} Pa·s. The conductance is given by:

$$C_{pump->atmosphere} = 182 \times \frac{0.3175[\text{cm}]^4}{5[\text{cm}]} \times \frac{760[\text{torr}] + 759.5[\text{torr}]}{2} = 281.0\text{L/s}$$

The conductance for the remaining segments of 1/4" ID Tygon and teflon tubing were calculated using the same methodology (Appendix D.1). The conductance for each segment is summarized in Figure 3.2.

Path	Connections	Tubing	Calculated Conductance
1	Pump to atmosphere	1/4" ID Tygon	281.0 L/s
2	Flow sensor to pump	1/4" ID Tygon	280.8 L/s
3	Valve manifold to flow sensor	1/4" ID Tygon	140.0 L/s
4	Valve manifold to flow sensor	1/8" ID nylon	10.05 L/s
5	Valve manifold	1/25" manifold bore	1.03 L/s
6	Valve manifold to ATD cartridge	1/8" ID nylon	16.74 L/s

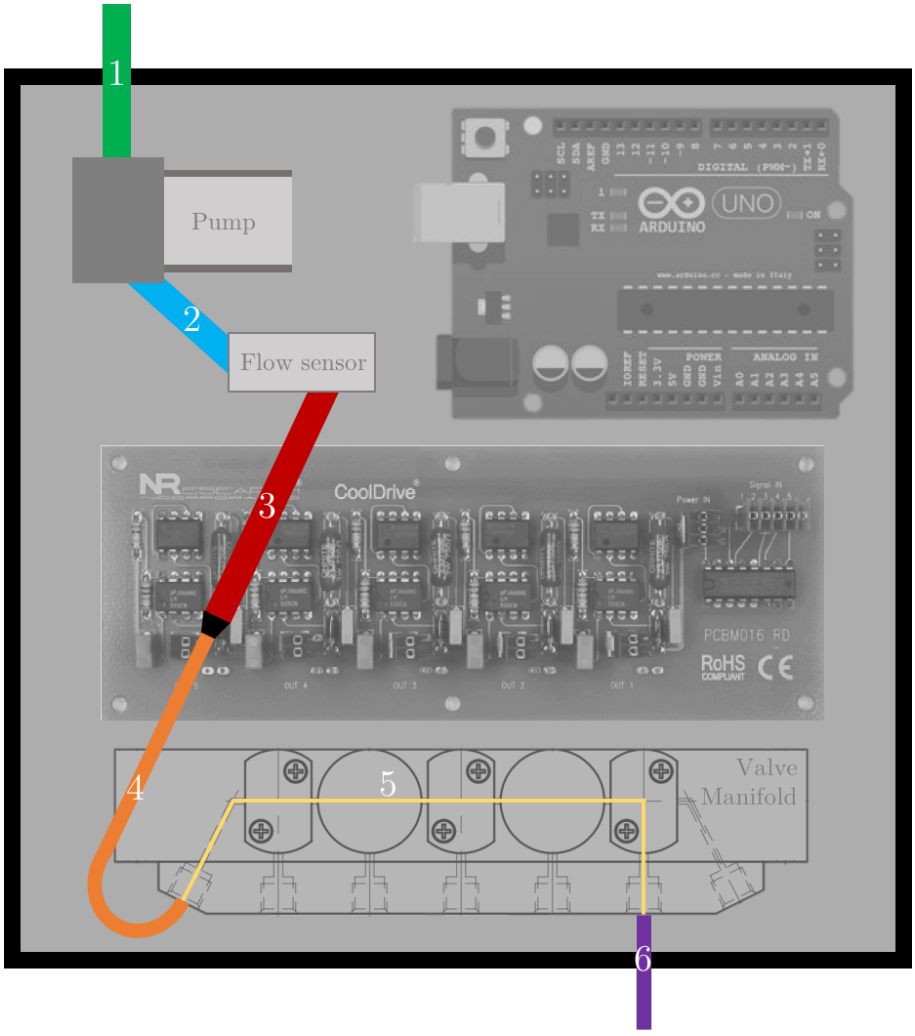

Fig. 3.2 **Calculated conductance for flow system tubing.** The tubing paths in the table correspond to the highlighted segments in the instrument schematic above. Air is pumped in from the sorbent tubes (connected to tube segment 6) and out of the tube segment 1.

Thus, the calculated pressure drop through the system can be determined:

$$\Delta P = \frac{Q}{C_{total}} = \frac{760 \text{ torr} \times 0.175\text{L/s}}{0.874\text{L/s}} = 152 \text{ torr}$$

This is a relatively small pressure drop caused by tubing conductance and is well within the operating specifications for the diaphragm pump installed on the sampling instrument to maintain a constant flow rate of 175 sccm.

3.2.2 Diaphragm Pump

The flow system is driven by a Parker CTS Micro Diaphragm pump (see Figure 3.6) (Appendix A.12), which delivers between 0.1 and 0.6 SLPM of flow from a compact form factor. The pump runs off of a 5.0 VDC brush sleeve bearing motor and barbed fittings allow for a leak-resistant interface with the 1/4" OD Tygon tubing. The volumetric flow for the pump is a function of the pressure drop across the inlet and outlet, as shown in the differential pressure vs. air flow graph in Figure 3.3. The pressure drop across the pump is controlled via an adjustable orifice valve at the output of the flow system.

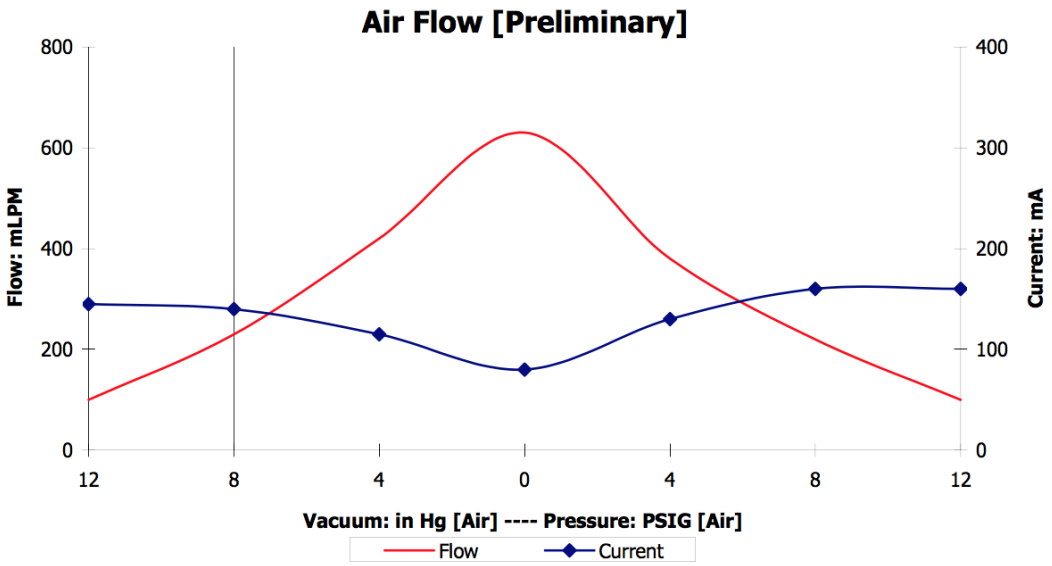

Fig. 3.3 **Nominal performance of diaphragm pump at 800' above sea level, 24°C, and at 5.0 VDC** [1].

3.2.3 Flow Sensor

The relationship between the atmospheric concentration and the mass of an analyte in a volume of air is derived from Avogadro's law. The result of this relationship is that, at room temperature and pressure, the molar volume of the vapor of a pure compound is 25 L mol^{-1}. For example, 25 L of pure benzene vapor would contain 1 mol (78 g) of benzene. Calculations for the mass of an analyte in a given volume of air, in terms of part per trillion (ppt) by volume, are therefore derived by considering the relative proportion of the volume of air sampled and the number of moles of the analyte. Thus, at room temperature and pressure, 25 L of air containing 1000 ppm (1 part in 1000) benzene would contain $\frac{1}{1000}$ mol (78 mg) of benzene. Likewise, 10 L of air containing 10 ppb (1 part in 10^8) benzene would contain $\frac{10}{25} \cdot \frac{1}{10^8}$ mol (310 ng) of benzene.

Utilizing this relationship allows for the calculation of the atmospheric concentration of an analyte from its mass on a sorbent tube:

$$\text{Concentration} = \frac{\text{Mass(g)}}{\text{Molar mass (g mol}^{-1})} \cdot \frac{25}{\text{Volume pumped through tube (L)}}$$

For example, if 10 L of air was pumped onto a sorbent tube and the mass of benzene collected was determined from gas chromatography data to be 3.2 μg, the atmospheric concentration would be:

$$\frac{3.2 \cdot 10^{-6}}{78} \cdot \frac{25}{10} = 1.0 \cdot 10^{-7} = 0.1 \text{ ppm}$$

Thus, measuring the volume of collected gas per sorbent tube is important for calculating accurate gas chromatography results. As such, an Omron mass flow sensor (see Figure 3.6) (Appendix A.9) was installed upstream of the pump to provide a continuous voltage signal corresponding to the mass flow at 0°C, 1 atmosphere. The mass flow rate can be converted into a volumetric flow rate in liters per minute using the measured pressure at the flow sensor and atmospheric temperature. The flow sensor supports a flow range of 0-1 SLPM and includes a built-in dust segregation system with cyclone flow structure, which diverts particulates from the sensor element. In addition to providing the volume of gas sampled (by integrating flow rate over time) required for gas chromatography analysis, the flow sensor also acts as an indicator of restricted flow due to foreign object debris entering the flow system during flight.

3.2.4 Pressure Sensor

An absolute pressure transducer (see Figure 3.6) was installed upstream of the flow sensor in order to measure the pressure drop across the diaphragm pump. Furthermore, the value reported by the pressure transducer can be used with atmospheric temperature to accurately convert mass flow rate to volumetric flow rate as the drone's altitude changes. The device supports a pressure range of 20 to 105 kPa and outputs a ratiometric voltage signal that can be converted linearly to a pressure value (Appendix A.11).

3.2.5 Valve Manifold

The valve manifold (NResearch Inc., 161T102) (Appendix A.8) consists of five independently actuated two-way, normally-closed solenoid valves. All five valves have a nominal orifice of 0.040 in and share a common output port. The manifold is controlled by a proprietary Cooldrive valve driver board designed and manufactured by NResearch Inc. (see Figure 3.6) (Appendix A.10). The board uses a holding voltage that is automatically achieved within 100 ms of activating the solenoid and independently controls the operation of the five solenoid valves using 5V logic level signals from the Arduino Uno microcontroller.

Each of the solenoid valves is actuated individually throughout a flight program. Original prototypes for the instrument included potential designs with a single solenoid valve and a custom mechanism for uncapping individual ATD cartridges during flight. However, the mechanical complexity of such an activation mechanism would likely introduce multiple failure modes with high probability, which would have a critical impact on achieving scientific goals. Furthermore, capping ATD cartridges during flights is unnecessary since sample collection by passive diffusion is negligible compared to that by active sampling at the target flow rate of 175 sccm. Past studies have shown that uptake by passive diffusion is only significant at extremely low flow rates (~1-4 sccm) [3].

3.2.6 Power Analysis

The upper bound of flight times offered by modern day drones is currently limited by the energy density of battery technology. In general, multi-rotor flight is extremely energy intensive, requiring significant power to reach cruising altitudes and handle turbulent flight conditions. As such, the design tradeoff between

using an external battery and siphoning power from the Matrice 600's set of six TB47S batteries has an immediate and important impact on meeting mission requirements. As shown in Figure 3.4, the pros and cons associated with both power options are quite convincing. Ultimately, the design decision hinges on the impact on total flight time, which directly determines the ability of the system to achieve the aforementioned scientific requirements.

	Pros	**Cons**
External Battery	- Fully isolated system - No power drain from flight functions	- Additional payload mass - Necessary to monitor and charge additional power source - Potential for battery to die during flight program
Onboard Battery	- No additional payload mass - Ability to monitor battery charge via DJI flight controller	- Will draw power directly from flight functions

Fig. 3.4 **Instrument power source decision table for external versus drone-based battery.**

Since the power consumption by the sampler instrument is independent of the power source, the current draw of the standard operating sequence for each sampling location was first calculated. The calculations are summarized in Table 3.1 below.

Table 3.1 Current draw from normal sampling operations.

Operation	Duration	Current Draw	mAh
Open valve	20 ms	200 mA	0.0011
Turn on flow sensor	5 min	20 mA	1.6667
Turn on pump for	5 min	150 mA	12.5000
Close valve	30 ms	200 mA	0.0017
			14.1695

For all five sampling sites, the total current draw of a complete flight program is

approximately:

$$14.1695 \text{ mAh} \times 5 \text{ tubes} = 70.85 \text{ mAh}$$

A 1.3 safety factor was used in order to account for current spikes, variances in consumption due to ambient temperature conditions, and performance inconsistencies based on manufacturing. This results in an estimated current draw per flight program:

$$70.85 \text{ mAh} \times 1.3 \text{ S.F.} = 92 \text{ mAh per 5 tubes}$$

External Battery

The effect of the additional mass of an external battery on flight time was first assessed. A linear fit on the payload vs. hovering time data from the Matrice 600's operating documentation was used to provide estimates on the reduced flight time as a result of the adding an external battery. As shown in Table 3.2, the Matrice 600 is capable of visiting five sampling sites while leaving ample flight time (~10 minutes) for inter-waypoint transits and departure/return to the mobile boat platform on the river. Assuming the drone travels at ~80% of its maximum forward speed (18 m/s), 10 minutes will allow for 10.8 kilometers to be covered. More importantly, the addition of a battery pack (assumed to be 0.45 lbs. based on popular commercial-off-the-shelf options) has a negligible impact on total flight time; the decrease in total flight time is roughly 50 seconds. Since the impact of an external battery pack on flight time is minimal for the Matrice 600, it was worth analyzing the expected performance of commercially available options. Specifically, for a commercial-off-the-shelf lithium polymer 2200mAh 11.1V battery pack:

$$\frac{2200 \text{ mAh capacity}}{92 \text{ mAh per flight}} = \sim 23$$

Thus, about 23 flights with sampling routines consisting of five ATD cartridge deployments can be achieved with a single, fully-charged 2200mAh battery pack. This is certainly a reasonable lifetime and will not require constant battery replacement for missions in the Amazon.

Table 3.2 Estimated flight performance for Matrice 600, external v. onboard battery.

ATD Cartridges per flight	Weight per ATD cartridge (lbs)	Volumetric Flow rate (sccm)	Sample volume per ATD cartridge	Sample time/tube (min)	Total sampling time (min)	Total mass (lbs)	Max flight time (min)	
							Onboard Battery	External Battery
1	0.025	200	1000	5	5	0.025	31.38	30.55
2	0.025	200	1000	5	10	0.05	31.33	30.51
3	0.025	200	1000	5	15	0.075	31.29	30.46
4	0.025	200	1000	5	20	0.1	31.24	30.42
5	0.025	200	1000	5	25	0.125	31.20	30.37
6	0.025	200	1000	5	30	0.15	31.15	30.33

Onboard Battery

The feasibility of drawing power directly from the Matrice 600 platform was also assessed. The power distribution board (PDB) on the chassis of the drone includes an XT30 connector providing 18VDC, typically for powering gimbal mounts and cameras. The PDB is powered by six TB47S batteries, each of which is rated at 4500 mAh. This results in a total rating of 27,000 mAh for the Matrice 600 at full charge. Assuming a maximum flight time of 35 minutes,

$$\frac{35 \text{ minutes}}{27{,}000 \text{ mAh}} = \frac{x}{26{,}908 \text{ mAh}}$$

$$x = 34.88 \rightarrow 6 \text{ sec. decrease in flight time}$$

While these estimates do not account for efficiencies and other sources of power consumption, it is clear that the power requirement for the sampling instrument is dwarfed by the power required for flight itself.

Design Decision

The calculations and estimates above suggest that the impact on flight time of an external battery pack is not significantly worse than siphoning power from the PDB of the Matrice 600. Both options result in reductions that are negligible when compared to the power consumption of the drone's own flight system. As such, the design decision hinges on factors such as ease of use and integration. In particular, an external battery pack allows for greater modularity and isolation from the drone platform itself. On the other hand, drawing power from the drone eliminates the need to charge and to monitor the status of a secondary power source, which could potentially be drained while a flight program is in progress, resulting in loss of data and wasted ATD cartridges. Since data collection and integrity are critical to achieving aforementioned scientific requirements, the final instrument design will be powered directly from the Matrice 600's PDB.

Further Considerations

It is also important to note that the battery tradeoff presented above is specific to the operating specifications of the Matrice 600 platform. While this is the most probable drone model to be used in upcoming sampling missions in Amazonia, it is worth considering the same battery tradeoff analysis for other drone platforms in order to provide the most flexible engineering design decisions. The same set

of estimates was performed on DJI's Matrice 100, another industry-grade drone offering reduced flight time and payload capabilities compared to the Matrice 600. Still, the Matrice 100 is capable of supporting the sampling instrument's mass and offers software features for defining GPS-specified sampling sites.

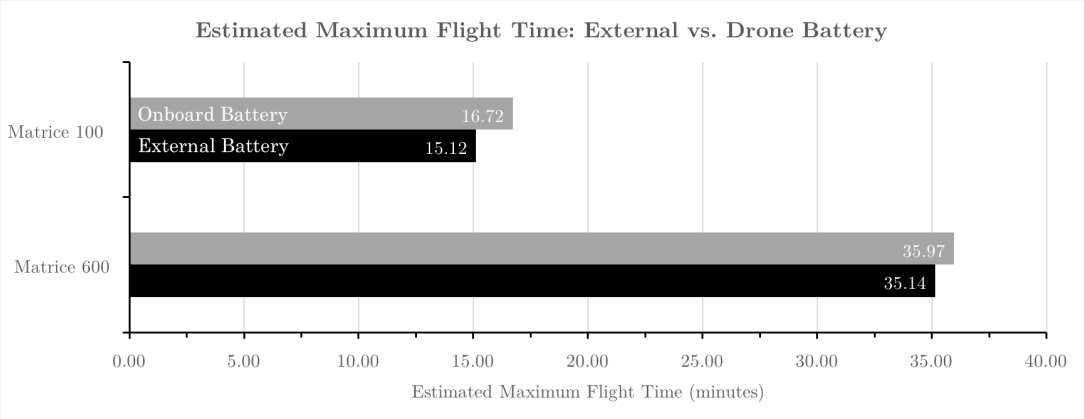

Fig. 3.5 **Estimated maximum flight times for Matrice 100 and Matrice 600 drone platforms.** Flight times are based on powering sampler instrument using external versus drone battery. Powering the sampler instrument with the onboard batteries results in slightly greater expected flight time for both platforms.

Table 3.3 shows the impact of an external battery (same specifications as the model used for Matrice 600 estimations) on the flight time of the Matrice 100. While the Matrice 100 is only able to support a flight with sampling from two ATD cartridges, the difference in flight time is roughly equal in magnitude to that experienced by the Matrice 600. In other words, adding an external battery does not significantly reduce the total flight time. The estimated flight time results for the Matrice 100 and 600 are summarized in Figure 3.5.

Table 3.3 Estimated flight performance for Matrice 100, external v. onboard battery.

ATD Cartridges per flight	Weight per ATD cartridge (lbs)	Volumetric Flow rate (sccm)	Sample volume per ATD cartridge	Sample time/tube (min)	Total sampling time (min)	Total mass (lbs)	Max flight time (min)	
							Onboard Battery	External Battery
1	0.025	200	1000	5	5	0.025	16.82	15.18
2	0.025	200	1000	5	10	0.05	16.73	15.10
3	0.025	200	1000	5	15.00	0.075	16.64	15
4	0.025	200	1000	5	20	0.1	16.55	14.91
5	0.025	200	1000	5	25	0.125	16.45	14.82
6	0.025	200	1000	5	30	0.15	16.36	14.73

Power Regulation

Two voltage regulators (one step-up and one step-down converter) draw 18VDC from the Matrice 600 power distribution board to provide 24VDC and 5VDC outputs to power the various components and sensors onboard the instrument. The step-up converter (used to provide the 24.0V voltage supply) supports converting a 3–34 VDC input voltage (with a maximum input current of 2.5A) to a continuously adjustable 4–35 VDC output voltage (with a maximum output current of 3.0A). On the other hand, the step-down converter (used to provide the 5.0V voltage supply) supports converting a 4–40 VDC input voltage (with a maximum input current of 2.0A) to a continuously adjustable 1.25–37 VDC output voltage (with a maximum output current of 2.0A). Both voltage regulators have a calibrated accuracy of 0.1V and include an LED display indicating the voltage output, which can be viewed through the transparent instrument housing prior to initiating flight programs.

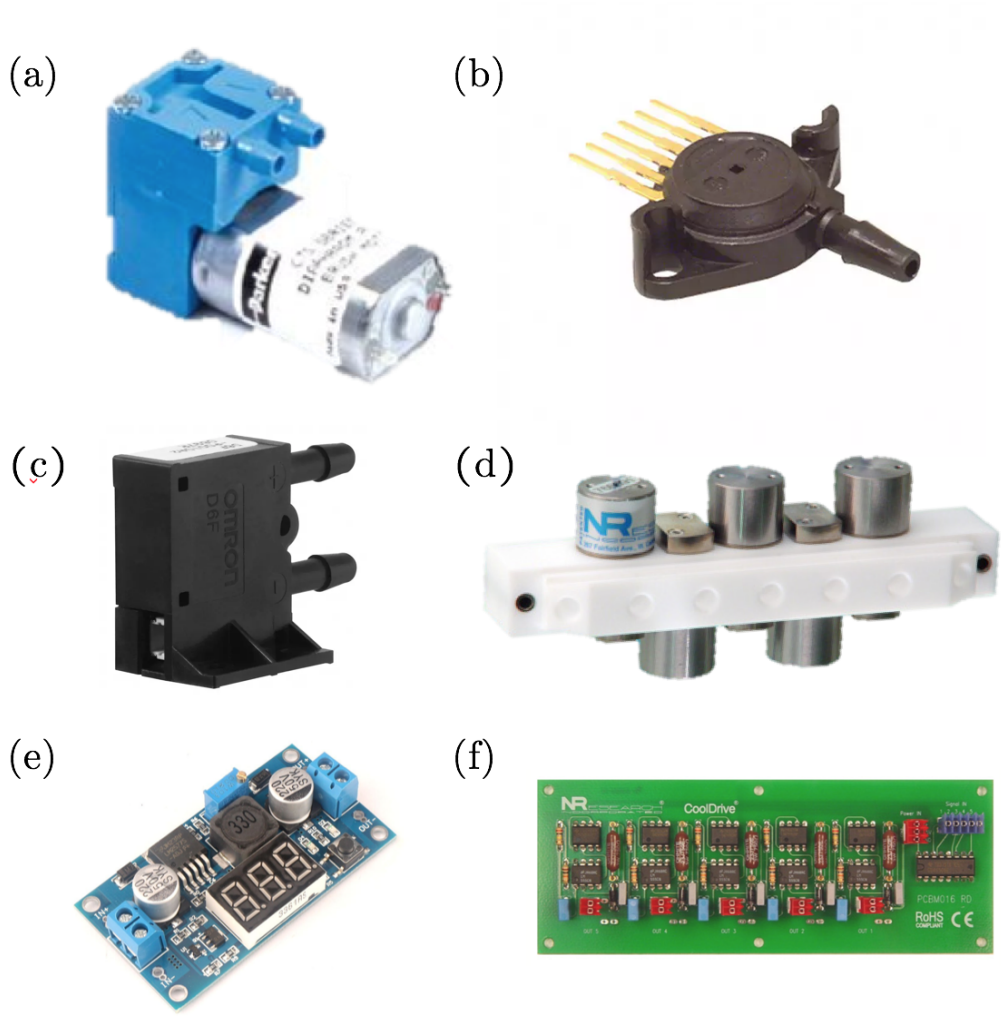

Fig. 3.6 **Select individual components.**(a) Mini-diaphragm pump, (b) pressure transducer, (c) mass flow sensor, (d) solenoid valve inline manifold, (e) voltage regulator, (f) solenoid valve driver board.

3.2.7 Component Activation Circuit

In order reduce power consumption during flight programs, a simple switching circuit was implemented to temporarily turn off the diaphragm pump and flow sensors. Specifically, these components can be deactivated while the drone is in transit between sampling locations, which can account for up to 30% of the flight program's duration. Moreover, turning off these components during non-hovering portions of the flight program can help reduce damage from mechanical shock and vibrations experienced during turbulent forward flight. The control code can also be easily modified to include a delay between turning on the pump and

opening a solenoid valve in order to reduce electrical transients. The circuit was implemented with a PN2222 transistor and 1N4001 diode along with Arduino code to control the switching itself. The full circuit diagram for the instrument is included in Appendix A.1.

3.2.8 Control and Data Logging Code

An Arduino Uno microcontroller is used to control the activation of the instrument, including:

1. Powering on the pump and flow sensors
2. Sequential activation of solenoid valves along the manifold
3. Flow and pressure data collection and storage to an onboard MicroSD card

The pseudocode for all three of these tasks (included in full in Appendix B) follows this general scheme:

Algorithm 1 Sequential Sampling Algorithm

```
procedure SEQUENTIAL SAMPLING
    A3-input ← signal from flight controller
    last-A3-input ← 0
    current-valve ← 1
    log-interval ← 2000 ms
    create new log file
    while power on do
        if A3-input != last-A3-input then
            if A3-input == HIGH) then
                turn on pump
                turn off pressure transducer
                turn on flow sensor
                open current-valve
                create new log
                wait for log-interval
                pressureReading ← analog voltage from pressure transducer
                flowReading ← analog voltage from flow sensor
                Save converted sensor readings and timestamp to log file
            else
                turn off pump
                turn off pressure transducer
                turn off flow sensor
                close current-valve
                current-valve = current-valve + 1
            end if
            lastA3-input ← A3-input
        else if A3-input == HIGH then
            wait for log-interval
            pressureReading ← analog voltage from pressure transducer
            flowReading ← analog voltage from flow sensor
            Save converted sensor readings and timestamp to log file
        end if
    end while
end procedure
```

Chapter 4

Assembly and Drone Integration

4.1 Instrument Housing

All instrument components were housed inside an enclosure designed to fit under the chassis of the Matrice 600. In particular, the size of the enclosure was constrained in order to avoid interference with the Matrice 600's landing legs an the depth of the enclosure was minimized in order to maintain the center of mass of the drone and eliminate negative impacts on flight dynamics. The housing was custom designed (see Appendices A.2 to A.5) and laser cut out of transparent acrylic to reduce mass and allow visibility to internal components, such as the voltage regulator displays. Large holes were added throughout the top, bottom, and side panels of the enclosure to reduce drag during flight and to also reduce the overall mass of the instrument. The majority of the components were mounted directly to the bottom panel of the enclosure using nylon 4-40, ½" screws, along with standoffs for circuit boards, as shown in Figure 4.1 and Figure 4.2. A custom mount was designed and 3D printed using a MakerBot to secure the diaphragm pump to the bottom panel (Appendix A.7). The operation of the solenoid valve manifold and diaphragm pump are not dependent on mounting orientation. In order to reduce the instrument mass, the individual panels of the enclosure were assembled with acrylic cement instead of using additional hardware.

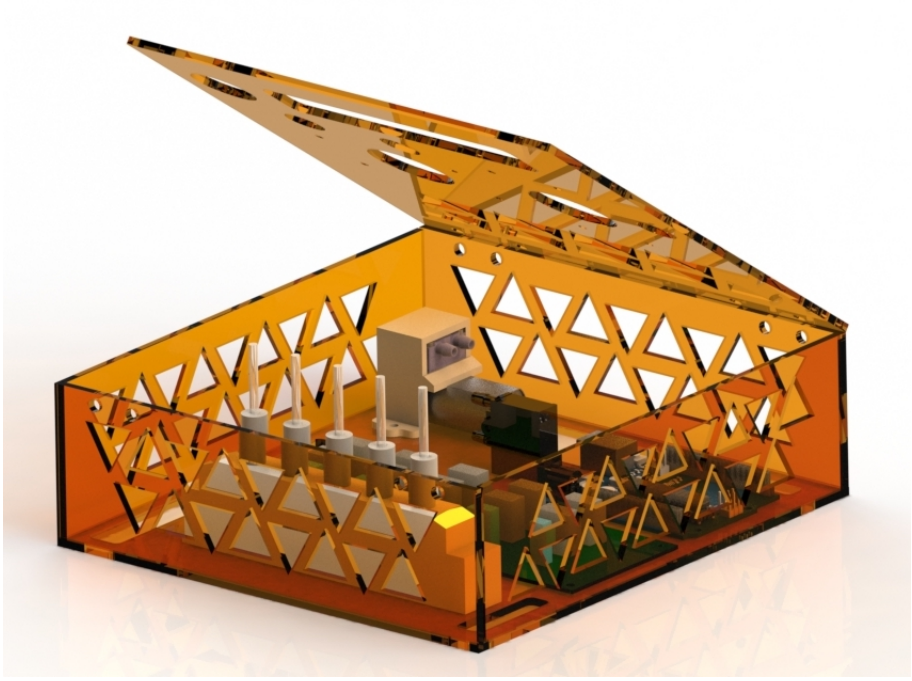

Fig. 4.1 **Rendering of instrument enclosure with valve manifold, pump, flow sensor, and driver board.**

The ATD cartridges extend outside of the enclosure to allow for easy access and replacement between consecutive flight programs. In addition, the top panel of the enclosure can be opened to access internal components (i.e. removing/inserting memory card).

4.2 Drone Integration

The enclosure was integrated with the Matrice 600 via the two expansion tubes on the underside of the drone chassis, as pictured in Figure 4.3. The expansion tubes, measuring 0.75” in diameter, are specifically designed for the addition of hardware (typically camera and gimbal mounts). Active locks designed for the Z15 Series Gimbal by DJI were used to clamp onto the expansion tubes and acrylic spacers were added (Appendix A.6) to lower the instrument and avoid mechanical interference with the landing leg motor boxes. M3x14mm screws were used to secure the instrument to the active locks. The mounting orientation of the instrument allows the ATD cartridges to hang vertically during flights and also allows the top panel of the enclosure to be opened while mounted.

Fig. 4.2 **Fully assembled sampler instrument.** The instrument enclosure is assembled out of acrylic with holes to reduce drag and mass. Individual components are mounted directly to the bottom panel of the enclosure and the top panel is designed to open for access to internal components.

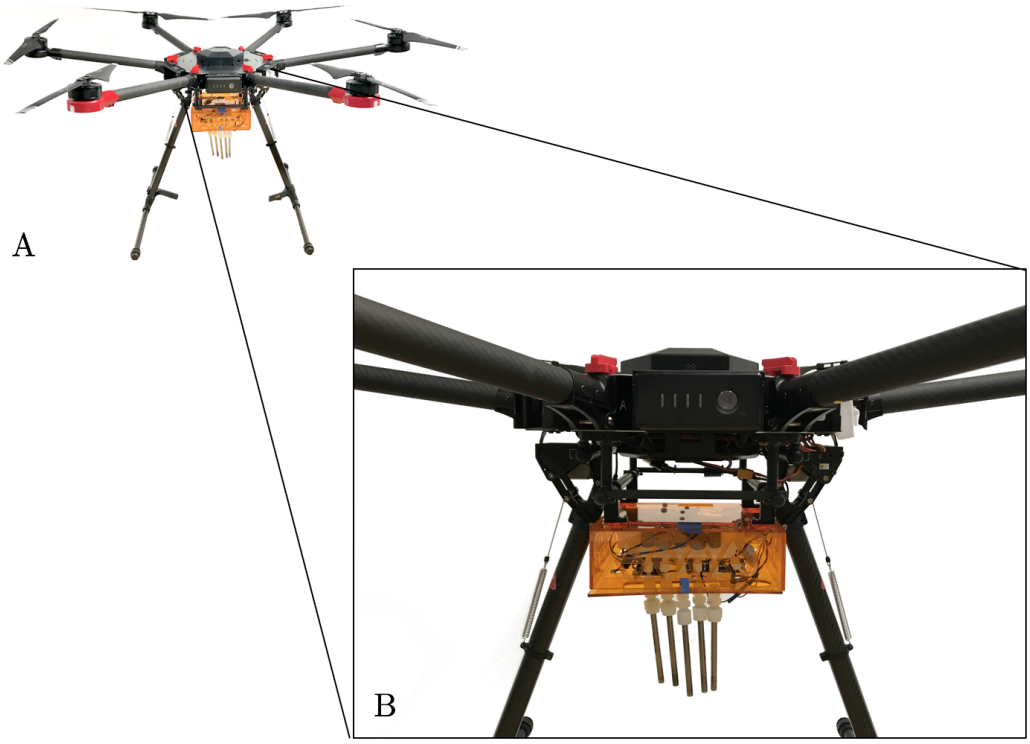

Fig. 4.3 **Mechanical integration of the the sampler instrument with Matrice 600 drone chassis.** The sample instrument is mounted directly to the two extension tubes on the underside of the drone body. The instrument enclosure does not interfere with the landing legs of the Matrice 600. ATD cartridges hang vertically from the instrument enclosure during flight for active sampling.

Chapter 5

System Validation

5.1 Sequential Valve Activation

Proposed flight plans within the Amazon will extend horizontally from riparian to several kilometers inland and vertically from near canopy to several hundred meters. Such sampling trajectories will allow specific sub-types of the rainforest to be targeted at scales of 1 km or less. Operation of the drones will take place from a boat that will be continuously re-positioned along the Amazon river system, allowing for sampling jobs spanning a range of different heterogeneous forest types in the Amazonia. Each flight program will include air sampling at multiple GPS waypoints; the number of sampling locations will vary based on the time spent traveling to and from the boat as well as between waypoints. As such, the ability for the flow system to sequentially cycle through multiple ATD cartridges is a first order scientific objective.

The sequential selection of ATD cartridges connected to the solenoid valve manifold and control via the Arduino microcontroller was validated using an oscilloscope to measure the output voltage from the flow sensor. The activation and deactivation of each valve was assessed to ensure that no differences existed in the sampling methodology for each ATD cartridge. As shown in Figure 5.1, the output voltage from the flow sensor is consistent across the five solenoid valves as each is cycled individually from open to closed. The system maintains a partial vacuum when all five solenoid valves are closed. Furthermore, the response time of the flow sensor voltage output as the solenoid valves are opened is nearly instantaneous (<0.1 sec.).

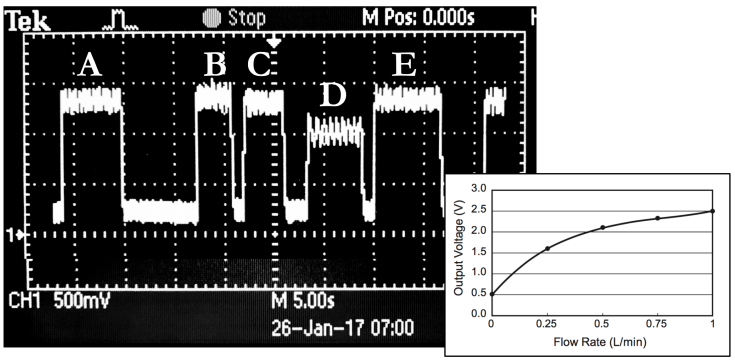

Fig. 5.1 **Flow sensor output for sequential manifold valve selection.** A-E high signals correspond to flow through individually opened manifold valves. Low signal shows low/no flow when all valves are closed. Note that the valve for signal D had a sample tube installed, which further constricted and therefore reduced the flow. Each subdivision on the y-axis is 500mV. Subfigure shows the characteristic curve for output voltage vs. flow rate for the onboard flow sensor.

5.2 Flow System Precision

The precision and accuracy of volumetric flow through each of the solenoid valves was also assessed. Since the duration of the sampling protocol at each GPS waypoint is controlled by the Matrice 600's flight computer, it is important that the volumetric flow rate through each valve be consistently repeatable in order to ensure that the volume of gas sampled at each GPS waypoint is roughly equal. While the volume of gas collected at each GPS waypoint need not be equal, consistency ensures that a time-based sampling protocol results in a representative sample volume for successful gas chromatography analysis.

The voltage output from the flow sensor was measured with an oscilloscope and the average value was recorded for 10 trials for each valve. Each of the trials lasted for a minimum of 10 seconds to allow for equilibrium flow. The same ATD cartridge was used across all trials in order to eliminate variances in conductance. As shown in Figure 5.2, the variance in flow rate through each valve was $<1\%$ the average voltage value. A slight linear decrease in flow towards ATD cartridge 5 can likely be attributed to the marginal decrease in conductance (solenoid valve 5 is the furthest from the common output port on the manifold). The difference in average flow rates between the five solenoid valves has no impact on scientific goals, since the volume of sampled gas per ATD cartridge is recorded and used

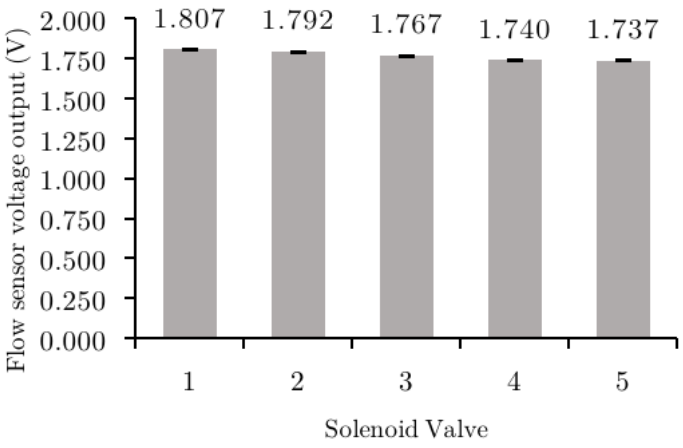

Fig. 5.2 **Flow sensor voltage output by valve.** The average voltage was recorded for 10 trials for each valve. Each trial lasted at least 10 seconds to allow for equilibrium flow and the same sample tube was used across all trials. The variance for each valve is <1% the average voltage value.

in each individual concentration calculation. Overall, the flow system exhibits high precision for each valve and accuracy across the manifold.

5.3 Flow Sensor Calibration

The mass flow sensor installed on the sampler instrument was calibrated using a mass flow controller (MKS Instruments Inc., 1179A Mass-Flo) in order to characterize the flow rate as a function of output voltage. The onboard flow sensor was installed at the output of the mass flow controller, which is rated for a full scale range of 1,000 sccm of nitrogen. The voltage output from the onboard flow sensor was then recorded at a 5 sccm step size for the 0 to 300 sccm range, which includes the flow rates mostly likely to be used for sampling missions in the Amazon rainforest. A coarser step size of 25 sccm was used for recording the flow sensor output in the 300 to 1,000 sccm range. The results of the calibration are shown in Figure 5.3.

5.4 Flow System Leakage Characterization

A flow leakage test was performed to detect and quantify the extent of volumetric leakage from the flow system. Since the flow sensor is located downstream from the ATD cartridges, leakage testing plays a critical role in ensuring the flow

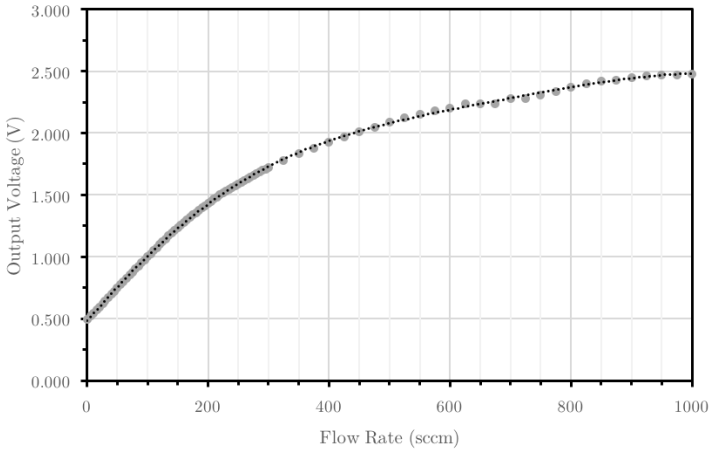

Fig. 5.3 **Flow calibration curve for onboard mass flow sensor.** The onboard flow sensor was calibrated againts a 1000 sccm nitrogen mass flow controller. The output voltage was recorded as a function of flow rate at 5 sccm steps for 0-250 sccm (the target flow rate range for VOC sampling) and at 25 sccm steps up to 1000 sccm.

sensor output can be used to derive an accurate measurement of the total volume of gas passed through each of the ATD cartridges. A mass flow sensor identical to the one installed on the instrument was placed at the input of the flow system, in place of the each of the ATD cartridges. Both flow sensors were powered from the instrument's 5.0 VDC voltage regulator and the voltage output from each was measured using an oscilloscope. Furthermore, the difference between the two flow sensors was recorded for a range of flow rates (controlled by an orifice valve at the output of the flow system) to assess change in leakage rate as a function of pressure drop across the system. The flow range for the test spanned from unimpeded flow (fully opened orifice valve) to the lowest attainable non-zero flow rate with the orifice valve and includes the target flow rate for sampling routines on future flight programs in the Amazon.

Figure 5.4 shows the difference in flow sensor outputs, hereafter referred to as the leakage value, as a function of the flow rate recorded by the onboard flow sensor unit for all five solenoid valves. A positive correlation exists between recorded flow rate and leakage value for all five valves. The dashed lines at +0.1 and -0.1V on the leakage value axis indicate the voltage accuracy range according to the manufacturer datasheet for the flow sensor model [2]. Furthermore, the shaded red region indicates the voltages that correspond to the flow rates that will likely

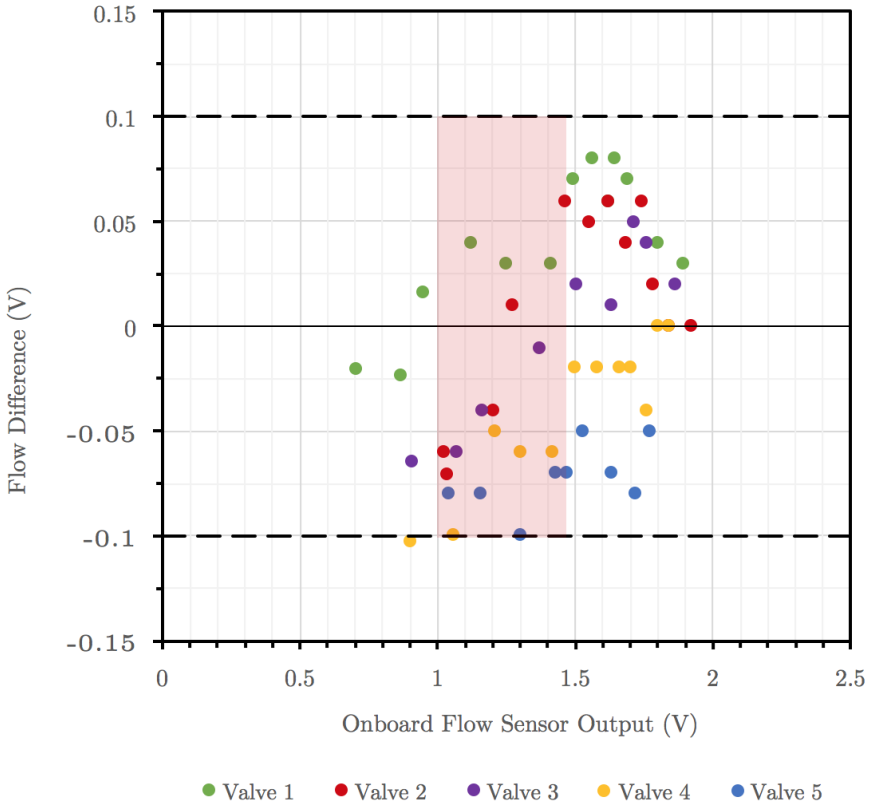

Fig. 5.4 **Quantification of flow system leakage.** Two identical mass flow sensors were used to quantify the leakage between each of the input valves and the diaphragm pump to ensure accurate volumetric measurements for post-flight gas chromatography analysis. The difference in voltage output from the flow sensors was measured as a function of onboard flow sensor reading. Dotted lines at $\pm$ 0.1 V indicate the accuracy range of the flow sensors while the shaded red zone indicates the target flow range for VOC sampling missions.

be used on used on flight programs in the Amazon (100-200 sccm). No data points within this flow range fall outside the bounds of the flow sensor's accuracy, suggesting that the leakage value can be attributed to sensor accuracy rather than true leakage through the flow system. Moreover, the leakage value for this flow range is roughly <= 5% the onboard flow sensor output.

5.5 Drone Test Flight

In order to validate the mechanical structure and assembly of the sampling instrument, several test flights were performed with the Matrice 600 platform. Five ATD cartridges were loaded onto the sampling instrument for the test flights, which took place at Danehy Park in Cambridge, Massachusetts, USA. Each test flight included a take off routine, various roll/pitch/yaw maneuvers during forward flight, fixed hovering, periods of rapid ascent and descent, and landing. The ambient conditions during the test flights were 0.5 °C with a mean wind speed of 22.5 km/h. The drone reached a maximum altitude of 119 m and speed of 46.8 km/h, traveling a cumulative total of 1.8 kilometers across all of the test flights.

Fig. 5.5 **Screenshot of sample test flight trajectory at Danehy Park, Cambridge MA from DJI Go application.** This particular test flight lasted 2:29 min, covering 656.7 m and reaching a maximum altitude of 38.0 m.

With the payload attached and six batteries at full charge, the DJI flight application reported an estimated total flight time of 40 minutes and 5 seconds. This estimate was calculated briefly after the first take off and is a function of the payload mass and wind conditions, among other parameters. The estimated flight time should be more than sufficient for proposed VOC surveys in the Amazon. A summary of a sample test flight is shown in Figure 5.5.

5.6 Simulated Flight Sampling Program

The A3 flight computer onboard the Matrice 600 does not support communication with external hardware components without custom applications built with DJI's Onboard SDK. As such, the software for a communication channel from the Matrice 600 platform to the sampling instrument was not completed for the scope of this project. However, the sequential sampling program and data logging process for future missions in the Amazon was simulated in the lab. Powering the sampler instrument from the 18VDC power supply on the Matrice 600's power distribution board, an external power supply was used to simulate a digital signal from the A3 flight controller to trigger sampling routines. Five ATD cartridges were loaded onto the sampling instrument and each each was sampled from for a minimum of five minutes to simulate potential flight programs in the Amazon. As shown in Table 5.1, the mean flow and pressure drop are consistent across all five ATD cartridges. Deviations in mean flow can likely be attributed to the difference in conductance of the individual ATD cartridges used in the test, which were previously used units.

Table 5.1 Summarized mean flow and mean pressure drop for simulated flight sampling program.

ATD Cartridge	Total Sampling Time (s)	Mean flow (sccm)	Mean pressure drop (atm)
1	318	175.0	0.024
2	354	174.1	0.024
3	306	177.5	0.024
4	320	192.2	0.024
5	384	188.3	0.024

5.7 In-flight Flow System Test

A final flight test was performed in order to validate complete instrument operation, including sequential valve activation and flow system function, with the drone in real flight conditions. In particular, it was important to verify whether or not the vibrations and forces experienced during flight would have any adverse effects on the function of the flow system. Since thermal desorption equipment was not available in the laboratory, completing the test with ATD cartridges was not possible. As such, colorimetric tubes (Sensidyne) were used in place of the ATD cartridges in order to qualitatively validate positive flow through the system. Water vapor tubes (1.7-33.8 mg/L) were selected for the relative abundance and fluctuation in water vapor in the ambient testing environment (Cambridge, Massachusetts).

The software on the Arduino Uno was adjusted in order to match the timing of sampling periods with the hovering/transit phases of the test flight. Since water vapor concentration is correlated with altitude, sampling took place within a vertical column at five altitudes: 20, 40, 60, 80, and 100 meters. While the colorimetric tubes are calibrated for use with a proprietary pump from the manufacturer (which samples 100mL over 20 seconds with non-constant flow), the sampling time was reduced to 30 seconds per altitude in order to best match the manufacturer recommended flow rate and volume.

The colorimetric tubes remained sealed until takeoff and were immediately collected and photographed at the end of the flight program in order to reduce the effects of ambient diffusion. The results of the test are shown in Figure 5.6. Color change (yellow to blue) is clearly visible in all five tubes, indicating that positive flow occurred through the flow system at each sampling altitude. This suggests that the sampler instrument is capable of functioning nominally in flight conditions. The rightmost tube is an unexposed control. Furthermore, a negative correlation between water vapor concentration and altitude is visible across the five colorimetric tubes. While these results are purely qualitative in nature due to the lack of calibration of the colorimetric tubes, the clear relationship between water vapor concentration and altitude is a promising result for similar flight tests to be carried out in the Amazon rainforest.

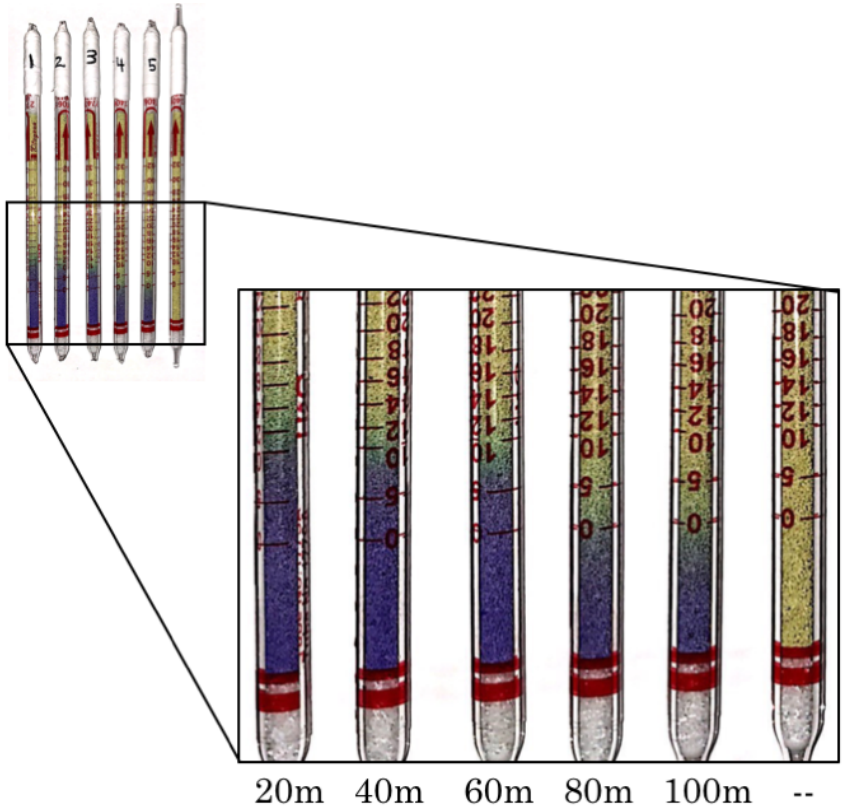

Fig. 5.6 **Colorimetric tubes for water vapor validate flow system function during flight conditions.** The color change in the tubes (yellow to blue) also indicates a negative correlation between altitude and water vapor concentration. The rightmost tube is an unexposed control.

Chapter 6

Conclusions and Future Work

6.1 Drone-based VOC sampling platform

Together with the flight capabilities of a drone platform (Matrice 600 in this case), the sampler instrument presented in this thesis will allow for accurate ambient measurements of the molecular identities and concentrations of volatile organics in previously inaccessible regions of tropical forests. Past studies aimed at addressing these fundamental scientific questions have been difficult in large part due to the coupled challenges of quantifying the immense biodiversity and a lack of a suitable approach for measuring emission variations over scales of 1km and less in height. A fleet of sampler-equipped drones dispatched from a mobile boat platform will provide new datasets to overcome these past challenges. Unlike previous methods based on single-point measurements, multiple drones offer a key new technology that enables sampling in a three-dimensional field, removing many of the earlier constraints imposed by direct measurements and reducing analytical uncertainties surrounding the magnitudes, variations, and processes controlling VOC emission and uptake at kilometer-scales. Specifically, these scientific measurements will provide important new data towards understanding the emission patterns and reaction pathways of VOCs.

The sampler instrument presented here has been shown to meet the operational specifications and consistency required for active sampling with analytical thermal desorption cartridges for gas chromatography. Powered directly from the drone platform and offering both sequential ATD cartridge activation and automated data logging, the sampler platform is a robust and reliable field-grade instrument.

6.2 Future Work

The deployment of the sampler instrument presented in this thesis is dependent on software integration with the Matrice 600 platform via DJI's software development kits (SDKs). As such, next steps will involve creating a custom application with DJI's mobile and onboard SDKs for the Matrice 600 platform in order to enable activation of the instrument in tandem with the drone's flight trajectory. In particular, the SDK will enable the drone platform to trigger the sequential activation of ATD cartridges at pre-programmed GPS-based sampling sites, as pictured in Figure 6.1. In practice, these samplings sites will be defined by longitude, latitude, and altitude. Furthermore, the drone would be capable of monitoring total sampling time per ATD cartridge. Alternatively, the flow rate data from the instrument could be sent to the drone's flight computer to trigger the start and stop of sampling based on the total volume sampled per ATD cartridge, with error protocols for handling flow system blockages (i.e. automatically skipping the current ATD cartridge in the event of blockage in order to avoid sampling past the allotted time). This second option would ensure that a representative volume of air for gas chromatography is achieved for each ATD cartridge.

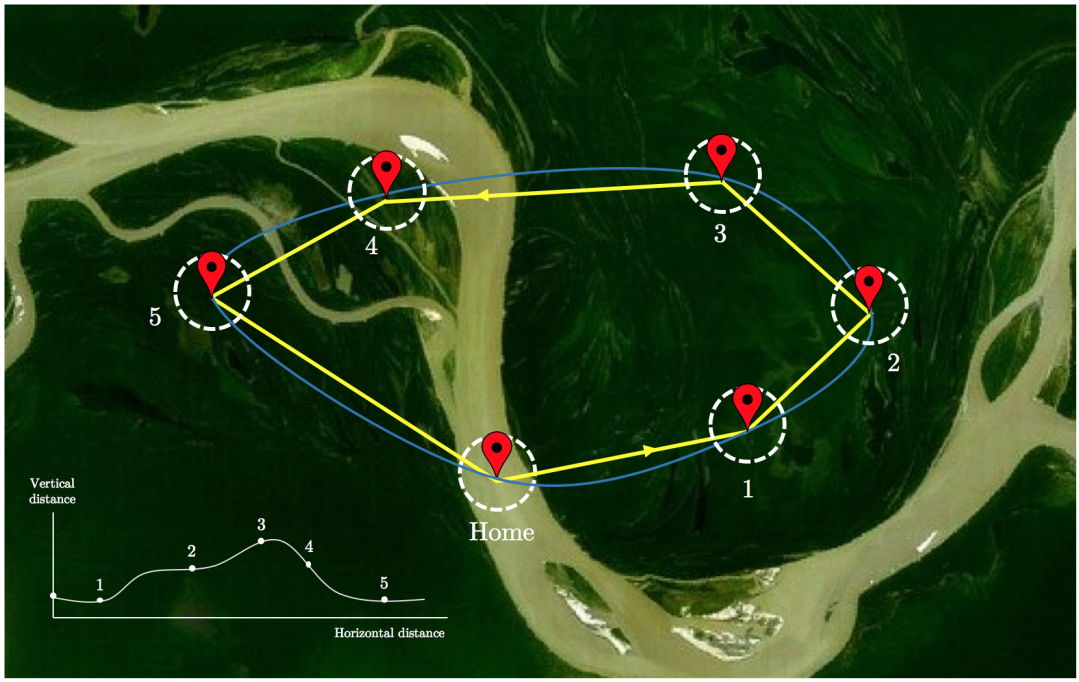

Fig. 6.1 **Sample flight program trajectory and sampling sites in the Amazon forest.** The home point will be a mobile boat platform on the river. The lower left corner shows the vertical travel for a sample flight.

In addition to integration with DJI's onboard SDK, the mobile SDK can be used to create a specialized flight application for use with a phone or tablet. This application would allow the user to create custom flight trajectories based on GPS waypoints and to also monitor the instrument status (i.e. flow rate, current ATD cartridge, etc.) during flight programs. Such a platform would offer an unprecedented level of control for collecting three-dimensional VOC concentration datasets in the Amazon. Specifically, flight programs - from take off and sampling at predefined waypoints to landing - would be executed completely autonomously from the mobile boat platform. With this system, researchers will be able to quickly deploy fleets of autonomous drones to simultaneously survey multiple sampling sites. The scientific findings from these missions in the Amazon - and other rainforests around the world - will provide insight into the emission patterns of VOCs at previously unexplored scales, ultimately helping to elucidate the complex photochemical pathways by which VOCs impact forest health and climate change.

References

[1] (2009). *CTS Diaphragm Pump, Brush Motor*. Parker Hannifin. Rev. C.

[2] (2017). *MEMS Flow Sensor*. Omron. Rev. 3.

[3] Batterman, S., Metts, T., and Kalliokoski, P. (2002). Diffusive uptake in passive and active adsorbent sampling using thermal desorption tubes. *Journal of Environmental Monitoring*, 4(6):870–878.

[4] Chang, C.-C., Wang, J.-L., Chang, C.-Y., Liang, M.-C., and Lin, M.-R. (2016). Development of a multicopter-carried whole air sampling apparatus and its applications in environmental studies. *Chemosphere*, 144:484–492.

[5] Fuentes, J. D., Gu, L., Lerdau, M., Atkinson, R., Baldocchi, D., Bottenheim, J. W., Ciccioli, P., Lamb, B., Geron, C., Guenther, A., Sharkey, T. D., and Stockwell, W. (2000). Biogenic hydrocarbons in the atmospheric boundary layer: A review. *Bulletin of the American Meteorological Society*, 81(7):1537–1575.

[6] Goldstein, A. H. and Galbally, I. E. (2007). Known and unexplored organic constituents in the earth's atmosphere. *Environmental Science Technology*, 41(5):1514–1521.

[7] Gu, D., Guenther, A., and Yu, H. (in press). Airborne observations reveal elevational gradient in tropical forest isoprene emissions. *Nature Communications*.

[8] Heagle, A. (1989). Ozone and crop yield. *Annual Review of Phytopathology*, 27(1):397–423.

[9] Heiden, A. C., Kobel, K., Wildt, J., Langebartels, C., and Schuh-Thomas, G. (2003). Emissions of oxygenated volatile organic compounds from plants part i: Emissions from lipoxygenase activity. *Journal of Atmospheric Chemistry*, 45(2):143–172.

[10] Langford, B., Misztal, P. K., Nemitz, E., Davison, B., Helfter, C., Pugh, T. A. M., Mackenzie, A. R., Lim, S. F., and Hewitt, C. N. (2010). Fluxes and concentrations of volatile organic compounds from a south-east asian tropical rainforest. *Atmospheric Chemistry and Physics*, 10(17):8391–8412.

[11] Mielke, L. H., Pratt, K. A., Shepson, P. B., Mcluckey, S. A., Wisthaler, A., and Hansel, A. (2010). Quantitative determination of biogenic volatile organic compounds in the atmosphere using proton-transfer reaction linear ion trap mass spectrometry. *Analytical Chemistry*, 82(19):7952–7957.

[12] Misztal, P. K., Owen, S. M., Guenther, A. B., Rasmussen, R., Geron, C., Harley, P., Phillips, G. J., Ryan, A., Edwards, D. P., Hewitt, C. N., and et al. (2010). Large estragole fluxes from oil palms in borneo. *Atmospheric Chemistry and Physics*, 10(9):4343–4358.

[13] Pankow, J. F., Luo, W., Melnychenko, A. N., Barsanti, K. C., Isabelle, L. M., Chen, C., Guenther, A. B., and Rosenstiel, T. N. (2012). Volatilizable biogenic organic compounds (vbocs) with two dimensional gas chromatography-time of flight mass spectrometry (gc × gc-tofms): sampling methods, vboc complexity, and chromatographic retention data. *Atmospheric Measurement Techniques*, 5(2):345–361.

[14] Patz, J. A., Campbell-Lendrum, D., Holloway, T., and Foley, J. A. (2005). Impact of regional climate change on human health. *Nature*, 438(7066):310–317.

[15] Sutherland, W. (2010). Plants: A different perspective.

[16] Williams, J., Yassaa, N., Bartenbach, S., and Lelieveld, J. (2007). Mirror image hydrocarbons from tropical and boreal forests. *Atmospheric Chemistry and Physics*, 7(3):973–980.

[17] Yassaa, N., Custer, T., Song, W., Pech, F., Kesselmeier, J., and Williams, J. (2010). Quantitative and enantioselective analysis of monoterpenes from plant chambers and in ambient air using spme. *Atmospheric Measurement Techniques*, 3(6):1615–1627.

Appendix A

Drawings and Schematics

VOC Sampler Instrument – Electrical Schematic

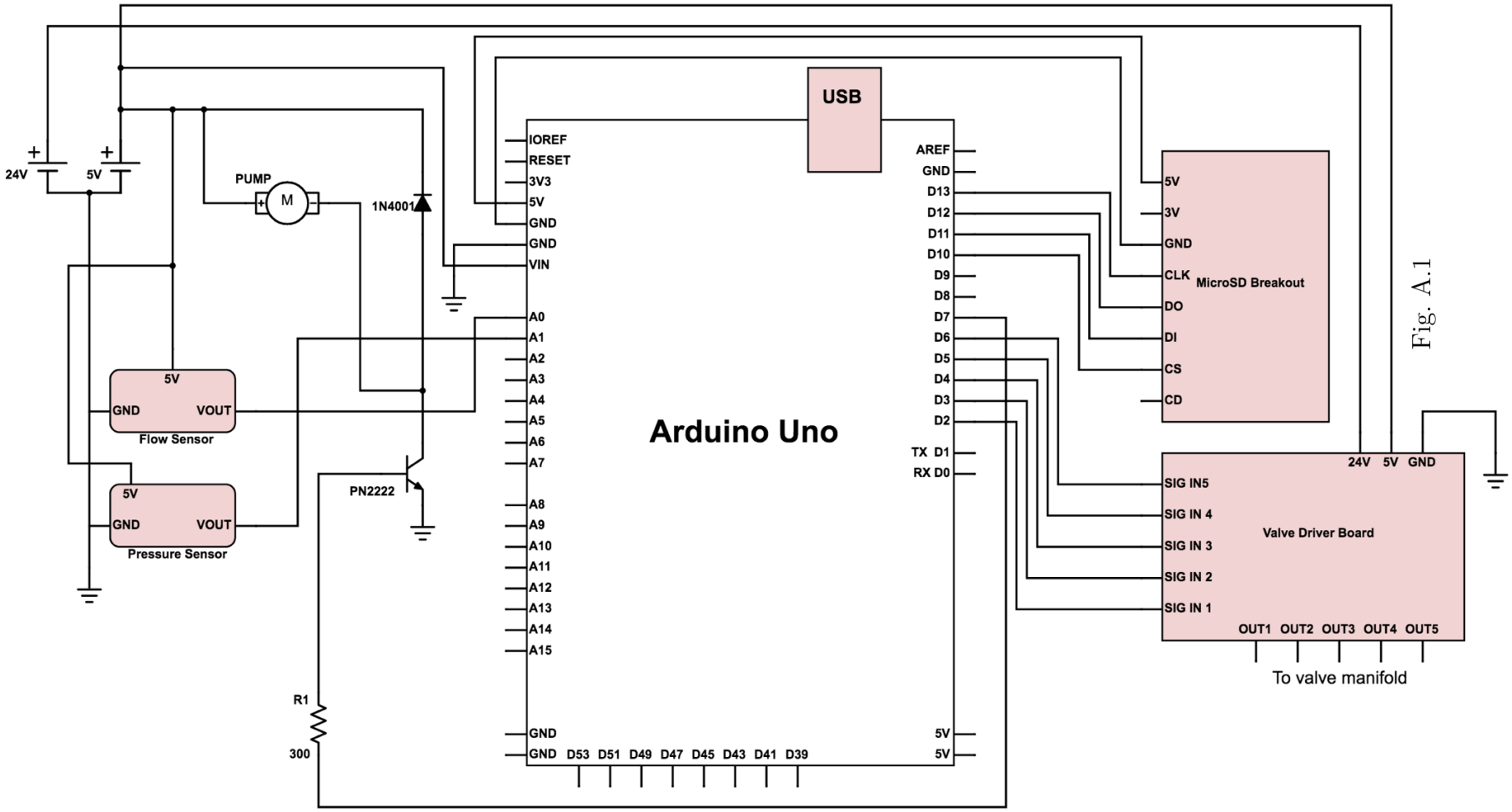

Fig. A.1

NOTES

1. All mounting holes are 0.125" diameter

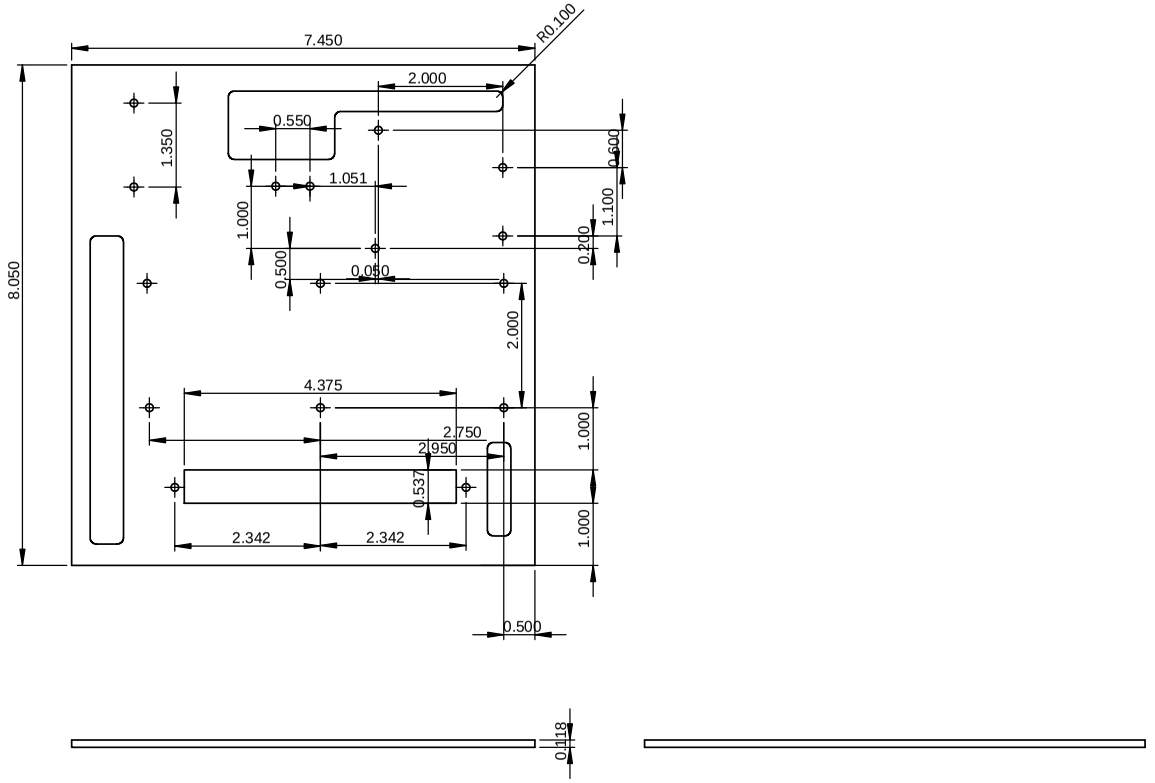

Fig. A.2

Material: **Acrylic**		This drawing and any information or descriptive material set out on it are the confidential and copyright property of ***Company Name***. © and MUST NOT BE DISCLOSED, COPIED, LOANED in whole or part or used for any purpose without the written permission of ***Company Name***.	Description: **Housing Bottom Panel**
Finish:			
Unless Otherwise Stated: Linear Tol.: **±0.2**, Angular Tol.: **0°15'** Surface Finish: **0.8µm** All Dimensions: **mm**		Document Type:	Drawn by: Daniel Wang / Drawn Date:
Drawing Scale: **1:2**			Checked/Approved by: / Checked/Approved Date:
Approx Weight: Kg	Drawing Produced In Accordance With: **BS8888**	Legal Owner: **Daniel Wang**	Part Number:
Projection Method: **THIRD ANGLE**	Sheet Size: **A3**		Drawing Number: / Sheet: **1 of 1** / Revision: **1**

NOTES

1. All triangles are equilateral

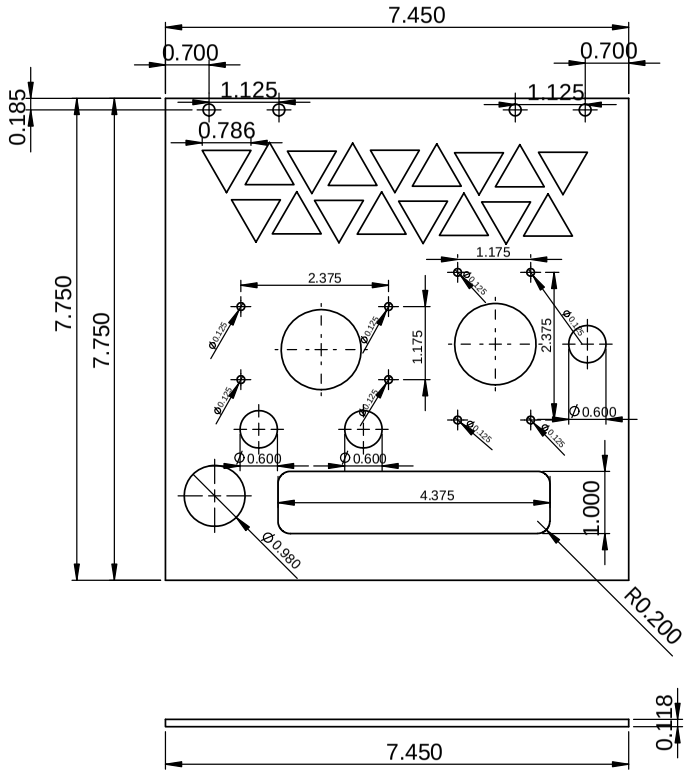

Fig. A.3

Material: Acrylic		This drawing and any information or descriptive material set out on it are the confidential and copyright property of ***Company Name***. © and MUST NOT BE DISCLOSED, COPIED, LOANED in whole or part or used for any purpose without the written permission of ***Company Name***.	Description: **Housing Top Panel**
Finish:			
Unless Otherwise Stated: Linear Tol.: **±0.2**, Angular Tol.: **0°15'** Surface Finish: **0.8µm** All Dimensions: **mm**		Document Type:	Drawn by: Daniel Wang / Drawn Date:
Drawing Scale: **1:2**			Checked/Approved by: / Checked/Approved Date:
Approx Weight:	Drawing Produced In Accordance With: **BS8888**	Legal Owner: Daniel Wang	Part Number:
Projection Method: **THIRD ANGLE**	Sheet Size: **A3**		Drawing Number: / Sheet: **1 of 1** / Revision: 1

NOTES

1. All triangles are equilateral

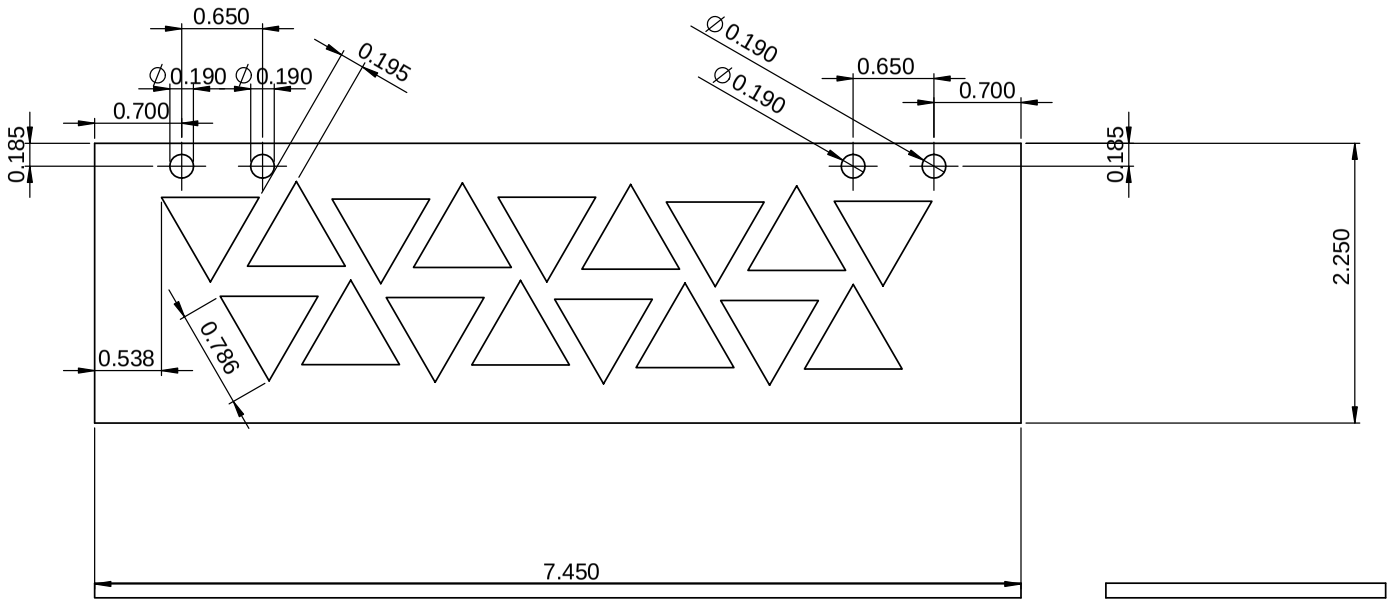

Fig. A.4

Material: Acrylic		This drawing and any information or descriptive material set out on it are the confidential and copyright property of ***Company Name***. © and MUST NOT BE DISCLOSED, COPIED, LOANED in whole or part or used for any purpose without the written permission of ***Company Name***.	Description: **Housing panel, Side 1**
Finish:			
Unless Otherwise Stated: Linear Tol.: **±0.2**, Angular Tol.: **0°15'** Surface Finish: **0.8µm** All Dimensions: **mm**		Document Type:	Drawn by: Daniel Wang / Drawn Date:
Drawing Scale: **1:1**		**Company Confidential**	Checked/Approved by: / Checked/Approved Date:
Approx Weight: Kg	Drawing Produced In Accordance With: **BS8888**	Legal Owner: Daniel Wang	Part Number:
Projection Method: **THIRD ANGLE**	Sheet Size: **A3**		Drawing Number: / Sheet: **1 of 1** / Revision: **1**

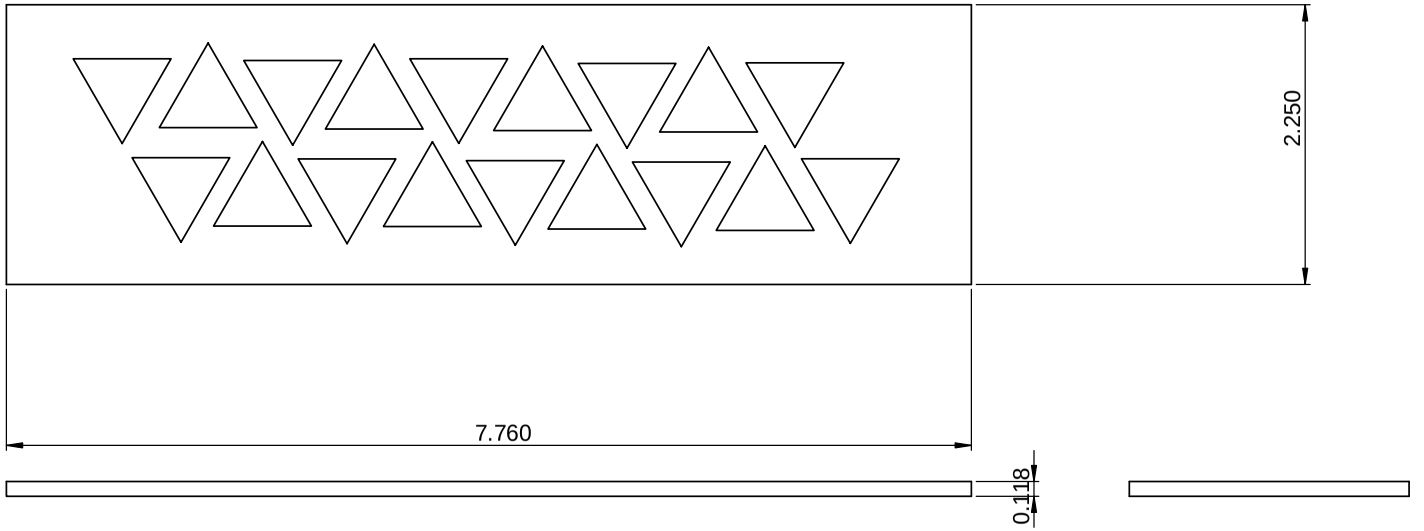

Fig. A.5

Material: Acrylic		This drawing and any information or descriptive material set out on it are the confidential and copyright property of ***Company Name***. © and MUST NOT BE DISCLOSED, COPIED, LOANED in whole or part or used for any purpose without the written permission of ***Company Name***.	Description: **Housing panel, side 2**
Finish:			
Unless Otherwise Stated: Linear Tol.: **±0.2**, Angular Tol.: **0°15'** Surface Finish: **0.8µm** All Dimensions: **mm**		Document Type:	Drawn by: Daniel Wang / Drawn Date:
Drawing Scale: **1:1**			Checked/Approved by: / Checked/Approved Date:
Approx Weight: Kg	Drawing Produced In Accordance With: **BS8888**	Legal Owner: **Daniel Wang**	Part Number:
Projection Method: **THIRD ANGLE**	Sheet Size: **A3**		Drawing Number: / Sheet: **1 of 1** / Revision: **1**

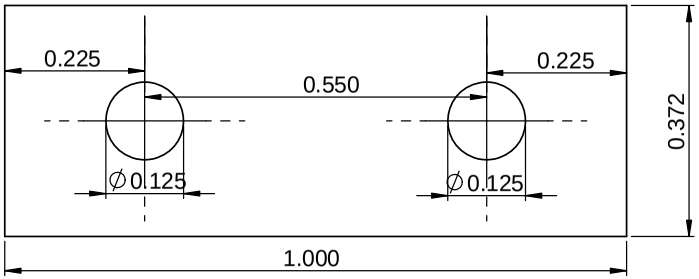

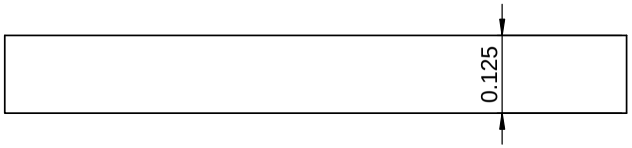

Fig. A.6

Material: **Acrylic**		This drawing and any information or descriptive material set out on it are the confidential and copyright property of ***Company Name***. © and MUST NOT BE DISCLOSED, COPIED, LOANED in whole or part or used for any purpose without the written permission of ***Company Name***.	Description: **Mounting spacer**
Finish: **n/a**			
Unless Otherwise Stated: Linear Tol.: **±0.2**, Angular Tol.: **0°15'** Surface Finish: **0.8µm** All Dimensions: **mm**		Document Type:	Drawn by: **Daniel Wang** / Drawn Date: **3/4/17**
Drawing Scale:			Checked/Approved by: / Checked/Approved Date:
Approx Weight: Kg	Drawing Produced In Accordance With: **BS8888**	Legal Owner: Daniel Wang	Part Number:
Projection Method: **THIRD ANGLE**	Sheet Size: **A3**		Drawing Number: / Sheet: **1 of 1** / Revision: **1**

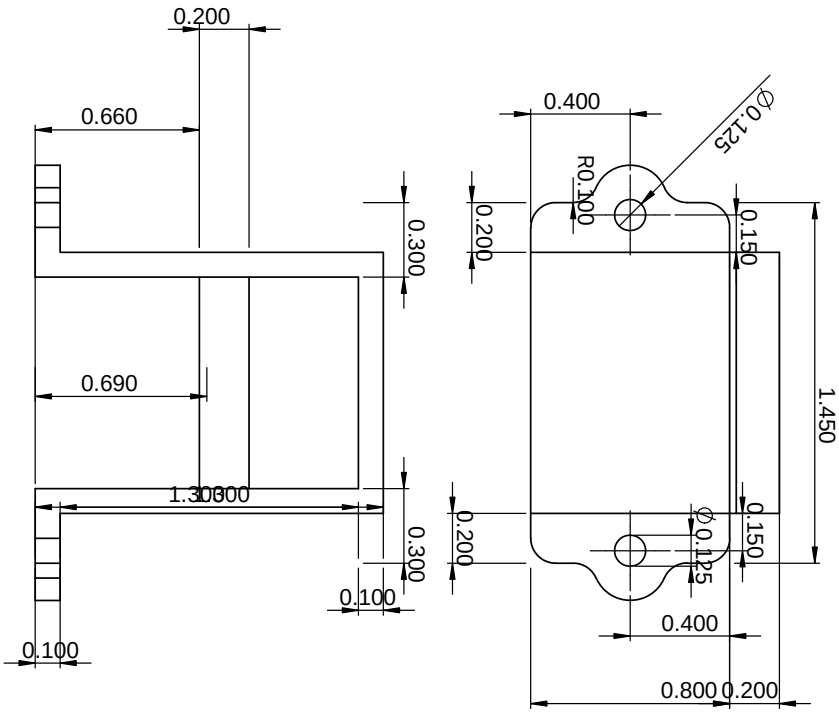

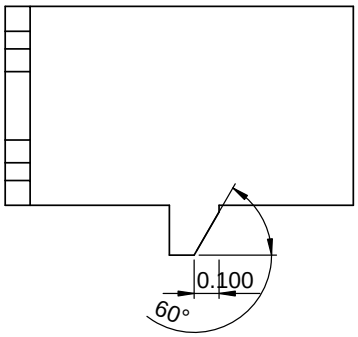

Material: PLA Filament	This drawing and any information or descriptive material set out on it are the confidential and copyright property of **Company Name** © and MUST NOT BE DISCLOSED, COPIED, LOANED in whole or part or used for any purpose without the written permission of **Company Name**.		Description: **Diaphragm Pump Mount**
Finish:			
Unless Otherwise Stated: Linear Tol.: **±0.2** Angular Tol.: **0°15'** Surface Finish: **0.8µm** All Dimensions: **mm**	Document Type:		Drawn by: Daniel Wang
Drawing Scale: **2:1**			Drawn Date:
Approx Weight: Kg	Legal Owner: Daniel Wang		Checked/Approved by:
Drawing Produced In Accordance With: **BS8888**			Checked/Approved Date:
Sheet Size: **A3**			Part Number:
Projection Method: **THIRD ANGLE**			Drawing Number:
			Sheet: **1 of 1**
			Revision: **1**

Fig. A.7

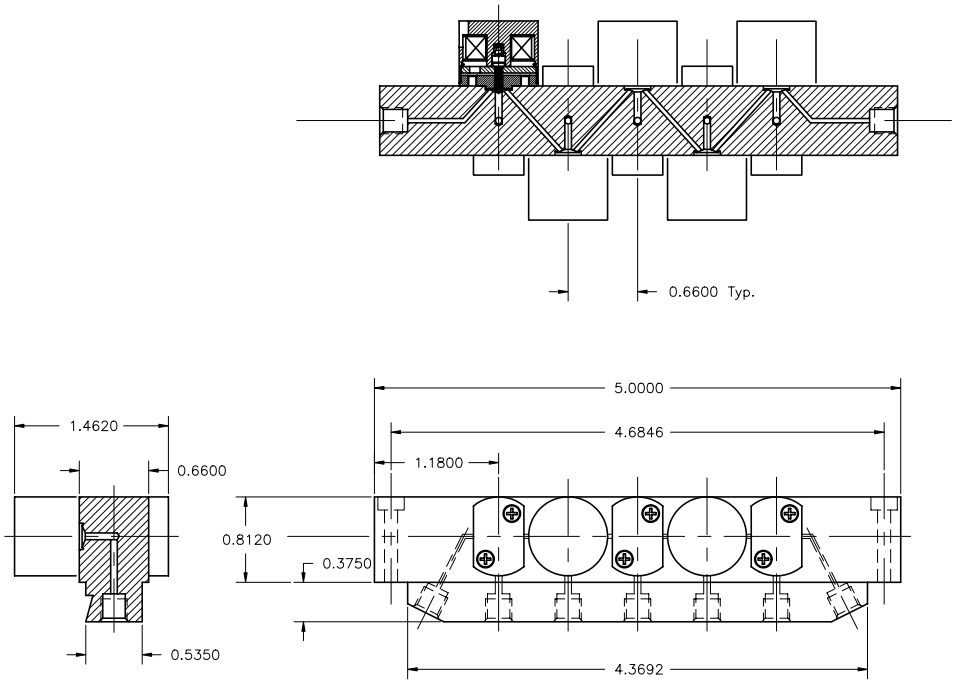

SPECIFICATIONS:

Mechanical: (Each Port)

TYPE:	2w Normally Closed
PORT CONNECTION:	1/4–28 Flat Bottom
NOMINAL ORIFICE:	0.040 In. (1.0 mm)
OPERATING PRESSURE:	Vacuum to 30 PSI (2 Bars)
TEST PRESSURE:	30 PSI N_2 (No leakage)
INTERNAL VOLUME:	269 microliters from bottom of ports.
WETTED MATERIALS:	TEFLON®
MOUNTING ORIENTATION:	Any Position

Electrical: (At 70° C No Pressure)

OPERATING VOLTAGE:	24 VDC (continous) 24 to 48 volts subject to duty cycle and/or holding voltage applied.
POWER CONSUMPTION:	1.15 Watts/24 VDC (approx.)
LEAD WIRES:	#26 AWG, TFE Insulated Blue 12 in. (305mm) long.
TEST VOLTAGE (ON):	< 18 VDC
TEST VOLTAGE (OFF):	1 to 8 VDC
RESPONSE TIME (ON):	20ms Max. (24 VDC) *5 to 20 ms subject to applied voltage and driving circuits.*
RESPONSE TIME (OFF):	30ms Max. (from 24 VDC) *30 to 5 ms adjustable by driving circuits.*

Fig. A.8

NOTE 1.)
Continouos rating applies to solenoid construction only. Since other materials incorporated in the product may not tolerate temperature variations as well as the solenoid application of holding voltage is strongly reccommended.

NOTICE:
This product is protected by one or more of the following United States Patents: 4,496,133; 4,993,456; 5,143,118; Re. 34,261 5,433,244. Other Patents Pending.

UNLESS OTHERWISE SPECIFIED			
Fractions	± 1/64	Break Sharp Edges	0.003–0.008
2 Pl. Dec.	± 0.005	All Small Fin. Radii	0.003–0.008
3 Pl. Dec.	± 0.002	All surfaces shall be Concentric,	
Angular	± 0.06°	Parallel, Flat, Square and True	
All Fin. Surf.		to Each Other within 0.001 T.I.R.	

Scale 1 : 1 (B)	Material As noted.	NR RESEARCH INCORPORATED	
Dr. By A. Sule	Date 07–19–1989		
Checked	Approved		
Part Name .161T102 5xNC 24vdc		Drawing Number .161V278	

OMRON

MEMS Mass Flow Sensor
D6F-P

A Compact, High-performance Flow Sensor with Dust Segregation Structure.

- Built in Dust Segregation System (DSS) with cyclone flow structure, diverts particulates from sensor element.
- High resolution and repeatability, even at low flow rates.
- Barbed ports with connector or PCB terminals, or manifold mount with connector versions.
- Built in voltage regulator, temperature compensation and amplified output. Measure up to 200 LPM with a bypass setup.
- High accuracy of ± 5% FS.
- RoHS Compliant

Ordering Information

Description	Case	Calibration Gas (See note 1.)	Flow Range	Mounting Method	Connection	Model
Flow Sensor	PBT	Air (See note 2.)	0-0.1 LPM	Flange mount	Lead terminals	**D6F-P0001A1**
			0-1 LPM			**D6F-P0010A1**
					Connector	**D6F-P0010A2**
				Manifold mount	Connector	**D6F-P0010AM2**
Cable Connector Assembly	- - -	- - -	- - -	- - -	- - -	**D6F-CABLE2**

Note: 1. Can be calibrated for different gas types. Consult your Omron representative.
2. Dry gas must not contain large particles, eg dust, oil, mist.
3. Cable Assembly "D6F-CABLE2", used with D6F-P0010A2 and D6F-P0010AM2, is sold separately.

Specifications

■ Characteristics

Models	D6F-P0001A1	D6F-P0010A1	D6F-P0010A2	D6F-P0010AM2
Flow Range (See note 1.)	0 to 0.1 L/min.	0 to 1 L/min.		
Calibration Gas (See note 2.)	Air			
Flow Port Type	barbed fitting maximum outside dia. 4.9 mm			manifold mount
Electrical Connection	Lead terminal		Connector (3 wire)	
Power Supply	4.75 to 9.45 VDC			
Current Consumption	Max. 15 mA (no load, Vcc = 5 VDC)			
Operating Output Voltage	0.5 to 2.5 VDC			
Output Voltage Limits (Min and Max.)	0 VDC min. and 3.1 VDC max. (Lead resistance 10 kΩ)			
Accuracy and Temperature Characteristics	± 5% F.S. max. of detected characteristics at 25 °C, within -10 to +60 °C (typical test results within ±2% F.S.)			
Repeatability (Reference (typical))	± 1.0% F.S.	± 0.4% F.S.		
Case Material	PBT			
Degree of Protection	IP40			
Withstand Pressure	50 kPa (7 psi)			
Pressure Drop (Reference (typical))	0.19 kPa			0.48 kPa
Operating Temperature	-10 to +60°C (1 LPM versions) and -33 to +75°C (0.1 LPM version) with no icing or condensation (Storage: -40 to +80°C with no icing or condensation)			
Operating Humidity	35 to 85% RH with no icing or condensation (Storage: 35 to 85% RH with no icing or condensation)			
Insulation Resistance	20 MΩ (500 VDC between lead terminal and the case)			
Dielectric Strength	500 VAC, 50/60 Hz for 1 minute. (Leakage current typ. Max. 1mA) between lead terminals and case.			
Weight	8.5 g			8.0 g
Response Time (Reference (typical))	150 msec			

Note: 1. Volumetric flow rate at 0°C, 101.3 kPa.
2. Dry gas. (must not contain large particles, dust, oil, mist)

Fig. A.9

CoolDrive™ Technical Information

Specifications	12 VDC (xx = 12)	24 VDC (xx = 24)
161D5Xxx	Power requirement at "V+" input: 94 mA min. for each Valve at 12 VDC Required Valve Solenoid coil resistance: 127 Ohms.	Power requirement at "V+" input: 48 mA min. for each Valve at 24 VDC Required Valve Solenoid coil resistance: 500 Ohms.
225D5Xxx	Power requirement at "V+" input: 133 mA min. for each Valve at 12 VDC Required Valve Solenoid coil resistance: 90 Ohms.	Power requirement at "V+" input: 70 mA min. for each Valve at 24 VDC Required Valve Solenoid coil resistance: 345 Ohms.
360D5Xxx	Power requirement at "V+" input: 353 mA min. for each Valve at 12 VDC Required Valve Solenoid coil resistance: 34 Ohms.	Power requirement at "V+" input: 171 mA min. for each Valve at 24 VDC Required Valve Solenoid coil resistance: 140 Ohms.
648D5Xxx	Power requirement at "V+" input: 600 mA min. for each Valve at 12 VDC Required Valve Solenoid coil resistance: 20 Ohms.	Power requirement at "V+" input: 308 mA min. for each Valve at 24 VDC Required Valve Solenoid coil resistance: 78 Ohms.

Signal IN (1 to 5): Logic Level Signal Inputs to control valve function. 1x5 pin header accepts AMP 3-644043-5 connectors.
Valve(s) are ON / Energized at High Input Level; OFF / not energized at Low Input Level.
Signal inputs must be connected to either High or Low level signals at all times.
No Floating / unconnected inputs allowed! Please connect inputs of unused channels to GND.
High Logic Level : 4 to 5.5 VDC; Low Logic Level : 0 to 1 VDC
Ground connection for signal inputs is at the Power IN connector (GND pin).

Power IN: Power Input Connections. 1x3 pin header accepts AMP 3-644042-3 connectors.
V+ : xx VDC (12 or 24 VDC), Power for connected Valves. See minimum current requirement in above chart.
+5V : 5 to 5.5 VDC, 150 mA min., Power for CoolDrive™ board
GND : Common ground for ALL power and signal connections.

Out (1 to 5): Output Connections to Valves. 5x2 pin headers accept AMP 3-644042-2 connectors.
The 2 pins on each 2 pin header are equal / reversible. Maximum available output current is 400 mA / channel, except for 648D5Xxx models, where it is 600 mA / channel.

Connectors, Wires, Crimping Tools: All required connectors are supplied with the CoolDrive™ boards (1x blue AMP 3-644043-5, 1x red AMP 3-644042-3, 5x red AMP 3-644042-2). The red connectors accept 22 AWG wires. The blue connector accepts 26 AWG wires. All wires with max. 0.06" (1.52 mm) insulation diameter. The AMP 58074-1 hand tool pistol grip is the recommended crimping tool in conjunction with the AMP 58246-1 head. For small volume applications more economical alternative may be the AMP 59803-1 maintenance tool.

WARNING: Please take extreme care while making connections as INPUTS and OUTPUTS are generally NOT protected against overvoltage / overcurrent / short circuit / reverse polarity, etc.

Mechanical: Mounting Holes: Use # 4-40 (3mm) Philister / Fillister Head Screws. Mounting Orientation: Any Position.

Dimensions

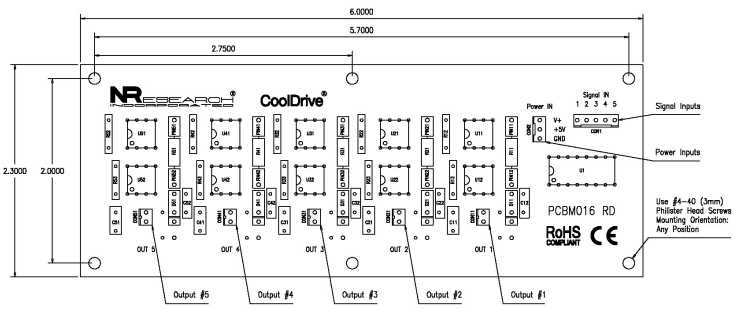

Fig. A.10

Operating Characteristics

Table 1. Operating Characteristics (V_S = 5.1 Vdc, T_A = 25°C unless otherwise noted, P1 > P2. Decoupling circuit shown in Figure 3 required to meet electrical specifications.)

Characteristic		Symbol	Min	Typ	Max	Unit
Pressure Range(1)		P_{OP}	20	—	105	kPa
Supply Voltage(2)		V_S	4.85	5.1	5.35	Vdc
Supply Current		I_o	—	7.0	10	mAdc
Minimum Pressure Offset @ V_S = 5.1 Volts(3)	(0 to 85°C)	V_{off}	0.225	0.306	0.388	Vdc
Full Scale Output @ V_S = 5.1 Volts(4)	(0 to 85°C)	V_{FSO}	4.816	4.897	4.978	Vdc
Full Scale Span @ V_S = 5.1 Volts(5)	(0 to 85°C)	V_{FSS}	—	4.59	—	Vdc
Accuracy(6)	(0 to 85°C)	—	—	—	±1.8	$\%V_{FSS}$
Sensitivity		V/P	—	54	—	mV/kPa
Response Time(7)		t_R	—	1.0	—	ms
Output Source Current at Full Scale Output		I_{o+}	—	0.1	—	mAdc
Warm-Up Time(8)		—	—	20	—	ms
Offset Stability(9)		—	—	±0.5	—	$\%V_{FSS}$

1. 1.0 kPa (kiloPascal) equals 0.145 psi.
2. Device is ratiometric within this specified excitation range.
3. Offset (V_{off}) is defined as the output voltage at the minimum rated pressure.
4. Full Scale Output (V_{FSO}) is defined as the output voltage at the maximum or full rated pressure.
5. Full Scale Span (V_{FSS}) is defined as the algebraic difference between the output voltage at full rated pressure and the output voltage at the minimum rated pressure.
6. Accuracy (error budget) consists of the following:

   Linearity: Output deviation from a straight line relationship with pressure over the specified pressure range.
   Temperature Hysteresis: Output deviation at any temperature within the operating temperature range, after the temperature is cycled to and from the minimum or maximum operating temperature points, with zero differential pressure applied.
   Pressure Hysteresis: Output deviation at any pressure within the specified range, when this pressure is cycled to and from the minimum or maximum rated pressure, at 25°C.
   TcSpan: Output deviation over the temperature range of 0 to 85°C, relative to 25°C.
   TcOffset: Output deviation with minimum rated pressure applied, over the temperature range of 0 to 85°C, relative to 25°C.
   Variation from Nominal: The variation from nominal values, for Offset or Full Scale Span, as a percent of V_{FSS}, at 25°C.
7. Response Time is defined as the time for the incremental change in the output to go from 10% to 90% of its final value when subjected to a specified step change in pressure.
8. Warm-up Time is defined as the time required for the product to meet the specified output voltage after the Pressure has been stabilized.
9. Offset Stability is the product's output deviation when subjected to 1000 hours of Pulsed Pressure, Temperature Cycling with Bias Test.

Fig. A.11

Mooresville, North Carolina 28117
T: 704-662-3500 F: 704-662-8744
www.hargravesfluidics.com

Part No.: **E155-11-050**
Model No.: **A.1F06N2.C05VDC**
Description: **CTS Diaphragm Pump, Brush Motor**

Dimensional Layout:

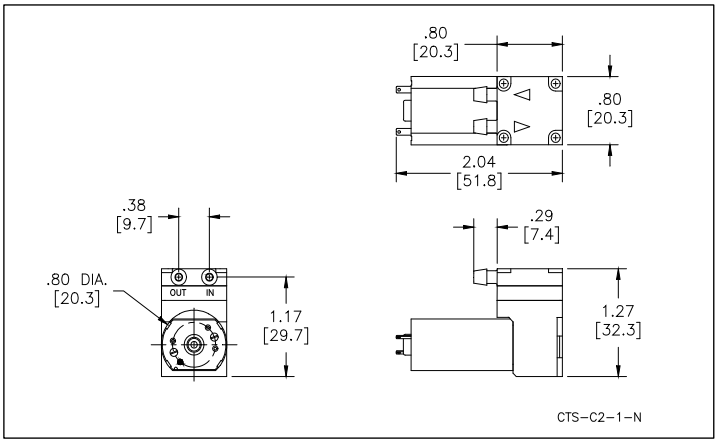

Specifications:

1. Wetted Materials:

Pump Head:	Polysulfone
Retainer Washer:	Polysulfone
Retainer Screw:	18-8 Stainless
Valves:	EPDM [65]
Diaphragm:	EPDM [F65]

2. Performance:

	Continuous	Maximum
- Pressure: PSIG [Air]	15.0	15.0
- Vacuum: in Hg [Air]	15.0	15.0

3. Electrical:

Motor:	Brush Sleeve Bearing
Operating Voltage:	5.0 VDC
In-rush Current:	5 x Operating Current for up to 50 ms
Recommended Fusing:	Slow Blow @ 2 x Operating Current

4. Other:

Temperature Range:	5 - 50° C
Free Flow RPM:	3130
Eccentric:	E350

5. Operating Limitations: N/A

6. Recommended Filtration: 40 Micron media w/ a minimum surface area of .24"Sq (152mmSq)

V / P	Flow	Current
12	100	145
8	230	140
4	420	115
0	630	80
4	380	130
8	220	160
12	100	160

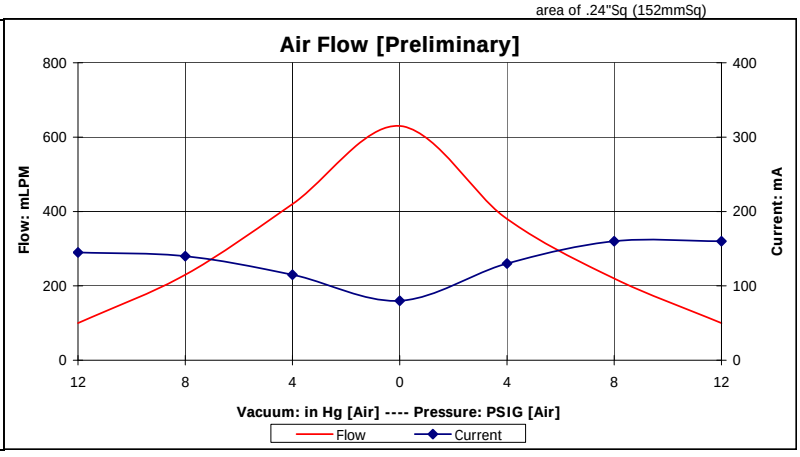

The above graph denotes nominal performance at 800' above sea level, 24°C, and at the specified voltage. **PR**

Fig. A.12

Appendix B

Software

```
/*
 * Sequential Valve Selection Program
 * with Datalogging to Arduino Uno breakout board
 * Daniel Wang, 2017
 *
*/
#include <Arduino.h>
#include <SPI.h>
#include <SD.h>
#include <Wire.h>
#include<stdlib.h>
#include <TimeLib.h>
//#include <DS1307RTC.h>  // a basic DS1307 library that
    returns time as a time_t
//#include <RTClib.h>

// A simple data logger for the Arduino analog pins
#define LOG_INTERVAL  2000 // mills between entries
#define ECHO_TO_SERIAL   1 // echo data to serial port
#define WAIT_TO_START    0 // Wait for serial input in
    setup()


// how many milliseconds before writing the logged data
    permanently to disk
```

```
// set it to the LOG_INTERVAL to write each time (safest)
// set it to 10*LOG_INTERVAL to write all data every 10
   datareads, you could lose up to
// the last 10 reads if power is lost but it uses less
   power and is much faster!
#define SYNC_INTERVAL 5*LOG_INTERVAL // mills between
   calls to flush() - to write data to the card
uint32_t syncTime = 0; // time of last sync()
// The analog pins that connect to the sensors
#define flowsensor 0            // analog 0
#define pressure 1              // analog 1
#define flight_comp 2           // analog 2

#define aref_voltage 5.0         // we tie 3.3V to ARef
   and measure it with a multimeter!


/*
   ************************************************************

 * ERROR HANDLING
 *
    ************************************************************
    */
//RTC_DS1307 RTC; // define the Real Time Clock object


// for the data logging shield, we use digital pin 10 for
    the SD cs line
const int chipSelect = 10;

// the logging file
File logfile;

void error(char *str)
{
  // print error the serial terminal
```

```
  Serial.print("error: ");
  Serial.println(str);

  while(1);
}

int out1 = 2;
int out2 = 3;
int out3 = 4;
int out4 = 5;
int out5 = 6;
int pump_v = 7;
int in1 = 8; // this is the input signal from the flight
   controller / drone
int LED = 13; // this is the built in indicator light
int currentPin = 2;

int A3_input = 0;          // current state of the button
int lastA3_input = 0;      // previous state of the button

// the setup function runs once when you press reset or
   power the board
void setup() {
  Serial.begin(9600); // open the serial port at 9600 bps
     :
  Serial.println();


  #if WAIT_TO_START
    Serial.println("Type any character to start");
    while (!Serial.available());
  #endif //WAIT_TO_START

  // initialize the SD card
  Serial.print("Initializing SD card...");
  // make sure that the default chip select pin is set to
  // output, even if you don't use it:
```

```
  pinMode(10, OUTPUT);

  // see if the card is present and can be initialized:
  if (!SD.begin(chipSelect)) {
    Serial.println("Card␣failed,␣or␣not␣present");
    // don't do anything more:
    return;
  }
  Serial.println("card␣initialized.");

  // create a new file
  char filename[] = "LOGGER00.CSV";
  for (uint8_t i = 0; i < 100; i++) {
    filename[6] = i/10 + '0';
    filename[7] = i%10 + '0';
    if (! SD.exists(filename)) {
      // only open a new file if it doesn't exist
      logfile = SD.open(filename, FILE_WRITE);
      break;  // leave the loop!
    }
  }

  if (! logfile) {
    error("couldnt␣create␣file");
  }

  Serial.print("Logging␣to:␣");
  Serial.println(filename);

    Wire.begin();



  logfile.println("millis,time,pressure_voltage,
      pressure_value_kpa,␣pressure_value_atm,␣
      pressure_drop_atm,␣flow_voltage,␣flow_value");
#if ECHO_TO_SERIAL
```

```
  Serial.println("millis,time,␣pressure_voltage,
      pressure_value_kpa,␣pressure_value_atm,␣
      pressure_drop_atm,␣flow_voltage,␣flow_value");
#endif //ECHO_TO_SERIAL


  // VALVE CONTROL STUFF
  // initialize digital pin LED_BUILTIN as an output.
  pinMode(LED_BUILTIN, OUTPUT);
  // initialize the digital output pins
  pinMode(2, OUTPUT);
  pinMode(3, OUTPUT);
  pinMode(4, OUTPUT);
  pinMode(5, OUTPUT);
  pinMode(6, OUTPUT);
  pinMode(7, OUTPUT);
  pinMode(in1, INPUT);
  digitalWrite(2, LOW);
  digitalWrite(3, LOW);
  digitalWrite(4, LOW);
  digitalWrite(5, LOW);
  digitalWrite(6, LOW);

}

// the loop function runs over and over again forever

// set up the global timer

void loop(void) {
  // read the signal from the flight computer
  A3_input = digitalRead(in1);

  if (A3_input != lastA3_input) {
    if (digitalRead(in1) == HIGH) { // if we get a high
        signal from the flight computer
```

```
digitalWrite(LED_BUILTIN, HIGH);    // turn the LED
   on as a visual indicator
digitalWrite(pump_v, HIGH);// turn on the pump
digitalWrite(currentPin, HIGH); // open the current
    solenoid valve

// wait for 5 seconds for the system to establish
   constant flow
delay(5000);


// BEGIN LOGGING DATA

// record the tube number
logfile.print("Sample Tube: ");
logfile.print(currentPin - 1);
logfile.println();
#if ECHO_TO_SERIAL
  Serial.print("Sample Tube: ");
  Serial.print(currentPin - 1);
  Serial.println();
#endif


// delay for the amount of time we want between
   readings
delay((LOG_INTERVAL -1) - (millis() % LOG_INTERVAL)
   );

// log milliseconds since starting
uint32_t m = millis();
logfile.print(m);           // milliseconds since
   start
logfile.print(", ");
#if ECHO_TO_SERIAL
  Serial.print(m);          // milliseconds since
     start
```

```
    Serial.print(",␣");
  #endif

  // fetch the time
  time_t t = now(); // store the current time in time
      variable t

  //DateTime now = RTC.now();
  //Serial.print(now);
  //Serial.println();
  // log time
  logfile.print("abs_time");
  /*
  logfile.print(now.year(), DEC);
  logfile.print("/");
  logfile.print(now.month(), DEC);
  logfile.print("/");
  logfile.print(now.day(), DEC);
  logfile.print(" ");
  logfile.print(now.hour(), DEC);
  logfile.print(":");
  logfile.print(now.minute(), DEC);
  logfile.print(":");
  logfile.print(now.second(), DEC);
  */
#if ECHO_TO_SERIAL
  Serial.print("abs_time");
#endif //ECHO_TO_SERIAL


// LOG SENSOR DATA
// note that analogRead() maps input voltages between
    0 and 5 volts into integer values between 0 and
   1023.
analogRead(flowsensor);
delay(10);
int flowReading = analogRead(flowsensor);
```

```
analogRead(pressure);
delay(10);
int pressureReading = analogRead(pressure);

// converting that reading to voltage, for 3.3v
   arduino use 3.3, for 5.0, use 5.0
float pressure_voltage = pressureReading *
   aref_voltage / 1024;
float pressure_value_kpa = ((pressure_voltage/5.09)
   +0.1518)/0.01059;
float pressure_value_atm = pressure_value_kpa
   *0.00986923;
float pressure_drop_atm = 1.0 - pressure_value_atm;

float flow_voltage = flowReading * aref_voltage /
   1024;
float flow_value = 0.2941*(flow_voltage)*(
   flow_voltage)*(flow_voltage) - 1.0436*(flow_voltage
   )*(flow_voltage) + 1.3547*(flow_voltage) - 0.4531;
//0.2941*(flow_voltage)^3 - 1.0436*(flow_voltage)^2 +
    1.3547*(flow_voltage) - 0.4531;

logfile.print(",␣");
logfile.print(pressure_voltage);
logfile.print(",␣");
logfile.print(pressure_value_kpa);
logfile.print(",␣");
logfile.print(pressure_value_atm);
logfile.print(",␣");
logfile.print(pressure_drop_atm);
logfile.print(",␣");
logfile.print(flow_voltage);
logfile.print(",␣");
logfile.print(flow_value);
```

```
#if ECHO_TO_SERIAL

  Serial.print(",␣");
  Serial.print(pressure_voltage);
  Serial.print(",␣");
  Serial.print(pressure_value_kpa);
  Serial.print(",␣");
  Serial.print(pressure_value_atm);
  Serial.print(",␣");
  Serial.print(pressure_drop_atm);
  Serial.print(",␣");
  Serial.print(flow_voltage);
  Serial.print(",␣");
  Serial.print(flow_value);
#endif //ECHO_TO_SERIAL


  logfile.println(); // add a new line to the log file
#if ECHO_TO_SERIAL
  Serial.println();
#endif // ECHO_TO_SERIAL


  }

  // turn off everything once the digital signal from
     the drone goes from high to low
  else {
    // sync all data to SD card
    syncTime = millis();
    logfile.flush();

    // power things down
    digitalWrite(LED_BUILTIN, LOW);
    digitalWrite(pump_v, LOW);// turn off the pump
    digitalWrite(currentPin, LOW); // close the current
        solenoid valve
```

```
      currentPin++;
      if (currentPin > 6) {
        currentPin = 2;
      }
    }
    lastA3_input = A3_input; //update the button state
  }
  else if (digitalRead(in1) == HIGH) { // for when there
     was no change in button state
// if the input signal is high, we want to continue
    recording data
      // BEGIN LOGGING DATA
      //DateTime now;

      // delay for the amount of time we want between
         readings
      delay((LOG_INTERVAL -1) - (millis() % LOG_INTERVAL)
         );



      // log milliseconds since starting
      uint32_t m = millis();
      logfile.print(m);           // milliseconds since
         start
      logfile.print(",");
      #if ECHO_TO_SERIAL
        Serial.print(m);          // milliseconds since
           start
        Serial.print(",");
      #endif

      // fetch the time
      //now = RTC.now();
      // log time
      logfile.print("abs_time");
      /*
```

```
    logfile.print(now.year(), DEC);
    logfile.print("/");
    logfile.print(now.month(), DEC);
    logfile.print("/");
    logfile.print(now.day(), DEC);
    logfile.print(" ");
    logfile.print(now.hour(), DEC);
    logfile.print(":");
    logfile.print(now.minute(), DEC);
    logfile.print(":");
    logfile.print(now.second(), DEC);
    */
#if ECHO_TO_SERIAL
    Serial.print("abs_time");
    /*
    Serial.print(now.year(), DEC);
    Serial.print("/");
    Serial.print(now.month(), DEC);
    Serial.print("/");
    Serial.print(now.day(), DEC);
    Serial.print(" ");
    Serial.print(now.hour(), DEC);
    Serial.print(":");
    Serial.print(now.minute(), DEC);
    Serial.print(":");
    Serial.print(now.second(), DEC);
    */
#endif //ECHO_TO_SERIAL


// LOG SENSOR DATA
// note that analogRead() maps input voltages between
    0 and 5 volts into integer values between 0 and
    1023.
analogRead(flowsensor);
delay(10);
int flowReading = analogRead(flowsensor);
```

```
analogRead(pressure);
delay(10);
int pressureReading = analogRead(pressure);

// converting that reading to voltage, for 3.3v
   arduino use 3.3, for 5.0, use 5.0
float pressure_voltage = pressureReading *
   aref_voltage / 1024;
float pressure_value_kpa = ((pressure_voltage/5.09)
   +0.1518)/0.01059;
float pressure_value_atm = pressure_value_kpa
   *0.00986923;
float pressure_drop_atm = 1.0 - pressure_value_atm;

float flow_voltage = flowReading * aref_voltage /
   1024;
float flow_value = 0.2941*(flow_voltage)*(
   flow_voltage)*(flow_voltage) - 1.0436*(flow_voltage
   )*(flow_voltage) + 1.3547*(flow_voltage) - 0.4531;
//0.2941*(flow_voltage)^3 - 1.0436*(flow_voltage)^2 +
    1.3547*(flow_voltage) - 0.4531;

logfile.print(",␣");
logfile.print(pressure_voltage);
logfile.print(",␣");
logfile.print(pressure_value_kpa);
logfile.print(",␣");
logfile.print(pressure_value_atm);
logfile.print(",␣");
logfile.print(pressure_drop_atm);
logfile.print(",␣");
logfile.print(flow_voltage);
logfile.print(",␣");
logfile.print(flow_value);
```

```
  #if ECHO_TO_SERIAL

    Serial.print(",␣");
    Serial.print(pressure_voltage);
    Serial.print(",␣");
    Serial.print(pressure_value_kpa);
    Serial.print(",␣");
    Serial.print(pressure_value_atm);
    Serial.print(",␣");
    Serial.print(pressure_drop_atm);
    Serial.print(",␣");
    Serial.print(flow_voltage);
    Serial.print(",␣");
    Serial.print(flow_value);
  #endif //ECHO_TO_SERIAL


    logfile.println(); // add a new line to the log file
  #if ECHO_TO_SERIAL
    Serial.println();
  #endif // ECHO_TO_SERIAL


  // Now we write data to disk! Don't sync too often -
     requires 2048 bytes of I/O to SD card
  // which uses a bunch of power and takes time
  if ((millis() - syncTime) < SYNC_INTERVAL) return;
  syncTime = millis();

  logfile.flush();


  }

}
```

Appendix C

Bill of Materials

Table C.1 Bill of Materials

Item	**Vendor**	**Source**	**Price (USD)**	**Quantity**	**Item Total**
Pump	Parker Hargraves	ES100 purchase	45	1	45
Nylon Tubing	Grainger	Faculty lab resources	0	1	0
Tygon Tubing	US Plastics Corp.	ES100 purchase	1.43	10	14.3
Valve manifold and driver board	NResearch Inc.	ES100 purchase	120	1	120
Orifice valve	US Plastics Corp.	ES100 purchase	6.1	1	6.1
Flow sensor	Omron	ES100 purchase	50	2	100
Flow sensor cable	Omron	ES100 purchase	11.63	2	23.26
Pressure transducer	Digikey	ES100 purchase	17.64	1	17.64
1/4" to 1/8" tubing fitting	Swagelok	ES100 purchase	8	5	40
Nylon Tubing Insert, 1/4 in. OD x 1/8 in. ID	Swagelok	ES100 purchase	1.4	3	4.2
Arduino Uno	Arduino	ALL supplied	0	1	0
Housing Acrylic	n/a	ALL supplied	0	1	0
Voltage converters	DROK	ES100 purchase	10	2	20
Mini breadboard	Digikey	ES100 purchase	4	1	4
					$394.5

Appendix D

Calculations

D.1 Flow System Conductance Calculations

$$C_{\text{pump->atmosphere}} = 182 \times \frac{0.3175[\text{cm}]^4}{5[\text{cm}]} \times \frac{760[\text{torr}] + 759.5[\text{torr}]}{2} = 281.0 \text{ L/s}$$

$$C_{\text{flow sensor->pump}} = 182 \times \frac{0.3175[\text{cm}]^4}{5[\text{cm}]} \times \frac{759.5[\text{torr}] + 759[\text{torr}]}{2} = 280.8 \text{ L/s}$$

$$C_{\text{valve manifold->flow sensor}} = 182 \times \frac{0.3175[\text{cm}]^4}{10[\text{cm}]} \times \frac{759[\text{torr}] + 758[\text{torr}]}{2} = 140.0 \text{ L/s}$$

$$C_{\text{valve manifold->flow sensor}} = 182 \times \frac{0.165[\text{cm}]^4}{10[\text{cm}]} \times \frac{758[\text{torr}] + 732[\text{torr}]}{2} = 10.05 \text{ L/s}$$

$$C_{\text{valve manifold bore}} = 182 \times \frac{0.1[\text{cm}]^4}{12[\text{cm}]} \times \frac{732[\text{torr}] + 627[\text{torr}]}{2} = 1.03 \text{ L/s}$$

$$C_{\text{sample tube->valve manifold}} = 182 \times \frac{0.165[\text{cm}]^4}{5[\text{cm}]} \times \frac{627[\text{torr}] + 614[\text{torr}]}{2} = 16.74 \text{ L/s}$$

$$\frac{1}{C_{total}} = \frac{1}{281.0} + \frac{1}{280.8} + \frac{1}{140.0} + \frac{1}{10.05} + \frac{1}{1.03} + \frac{1}{16.74} \rightarrow C_{total} = 0.874 \text{ L/s}$$